

1N-61-ER  
153284

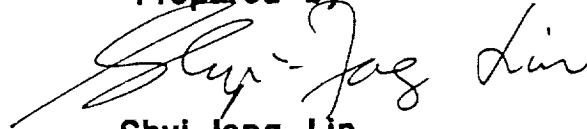
**Development of Code Evaluation Criteria for  
Assessing Predictive Capability and Performance**

**Contract Number NAS8-38858**

**Final Contract Report  
March 1993**

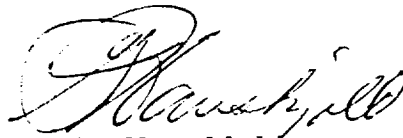
**Prepared for  
NASA Marshall Space Flight Center  
Huntsville, Alabama 35812**

**Prepared by**



**Shyi-Jang Lin  
Principal Investigator**

**Approved by**



**G. Havskjold  
Program Manager**

(NASA-CR-192~~552~~) DEVELOPMENT OF  
CODE EVALUATION CRITERIA FOR  
ASSESSING PREDICTIVE CAPABILITY AND  
PERFORMANCE Final Report, Mar. 1991  
- Mar. 1993 (Rockwell  
International Corp.) 47 p

N93-24473

Unclas

G3/61 0153284

## **ACKNOWLEDGEMENTS**

This work was supported by the NASA Marshall Space Flight Center under contract number NAS8-38858, and was monitored by Mr. Joe Ruf. The authors would also like to express their appreciation to Mr. Daniel C. Chan, both for consultation on use of the REACT CFD code and for computations of Phase 2 validation cases.

## TABLE OF CONTENTS

	<u>Page</u>
<b>ACKNOWLEDGEMENTS</b>	ii
<b>LIST OF ILLUSTRATIONS</b>	iv
<b>LIST OF TABLES</b>	iv
<b>ABSTRACT</b>	1
<b>1.0 INTRODUCTION</b>	1
1.1 Code Validation Classifications	3
1.2 Code Evaluation	5
1.3 Error Assessment	6
1.4 Criteria for Selection of Code Validation	8
<b>2.0 CFD CODE VALIDATION PROCEDURE</b>	11
2.1 Phase 1 – Unit Problems	12
2.2 Phase 2 – Benchmark Cases	13
2.3 Phase 3 – Simplified Partial Flowpath	13
2.4 Phase 4 – Actual Hardware	14
2.5 Incrementally Extending Code Validation	14
<b>3.0 DEMONSTRATION OF THE CODE VALIDATION PROCEDURE</b>	14
3.1 Code and Application Selected	14
3.1.1 Identify Code to be Validated	15
3.1.2 Select Final Application and Decompose Over Four Phases	16
3.1.3 Establish Code Evaluation Criteria	19
3.2 Code Validation Procedures Results	20
3.2.1 Phase 1 – Straight Duct	20
3.2.2 Phase 2 – Square Duct with 90° Elbow	24
3.2.3 Phase 3 – 3-D Turbine Cascade	26
3.2.4 Phase 4 – SSME HPFTP	28
<b>4.0 SUMMARY</b>	41
<b>5.0 REFERENCES</b>	42

## LIST OF ILLUSTRATIONS

<u>Figure No.</u>	<u>Title</u>	<u>Page</u>
1	Four Phase Code Validation Procedure	12
2	Building Block Approach to Develop Validation database	15
3	Successive Composition of Impeller	17
4	SSME HPFTP Impeller	17
5	Streamwise Velocity Profiles for Coarse and Fine Grid Computations	22
6	Streamwise Velocity Profiles for Single and Two-Zone Computations	22
7	Velocity Contours for Nonsmooth and Smoother Zonal Interfaces	23
8	Convergence History for 1- and 2-Zone Duct Flow	23
9	Flow Configuration for Square Duct with 90° Elbow	24
10	Velocity Profiles at 77.5° Location	25
11	Numerical Error and Secondary Flow at 60° Location	27
12	Blade Passage Grids for "H" and "O-H" Topologies	29
13	Static Pressure Distribution on Coarse Grids	29
14	Static Pressure Distribution on Fine Grids	30
15	Impeller Grid Topology (30K Grid Solution)	31
16	Comparison of CFD Solution to Test Data - Plane 1	34
17	Comparison of CFD Solution to Test Data - Plane 3	35
18	Test Data versus 30K Grid Solution - Plane 1	37
19	Test Data versus 90K Grid Solution - Plane 1	38
20	Test Data versus 30K Grid Solution - Plane 3	39
21	Test Data versus 90K Grid Solution - Plane 3	40

## LIST OF TABLES

<u>Table No.</u>	<u>Title</u>	<u>Page</u>
1	Generic Representation of Criteria for Three Validation Phases	6
2	Impeller Design Criteria for Three Validation Phases	20
3	Impeller Flow Split Comparison	33

# **DEVELOPMENT OF EVALUATION CRITERIA AND A PROCEDURE FOR ASSESSING PREDICTIVE CAPABILITY AND CODE PERFORMANCE**

S. J. Lin, S. L. Barson, M. M. Sindir, and G.H. Prueger

## **ABSTRACT**

Computational Fluid Dynamics (CFD), because of its unique ability to predict complex three-dimensional flows is being applied with increasing frequency in the aerospace industry. Currently, no consistent code validation procedure is applied within the industry. Such a procedure is needed to increase confidence in CFD and reduce risk in the use of these codes as a design and analysis tool. This final contract report defines classifications for three levels of code validation, directly relating the use of CFD codes to the engineering design cycle. Evaluation criteria by which codes are measured and classified are recommended and discussed. Criteria for selecting experimental data against which CFD results can be compared are outlined. A four phase CFD code validation procedure is described in detail. Finally, the code validation procedure is demonstrated through application of the REACT CFD code to a series of cases culminating in a code to data comparison on the Space Shuttle Main Engine High Pressure Fuel Turbopump Impeller.

## **1.0 INTRODUCTION**

Applications such as the National Launch System (NLS), the National Aero-Space Plane (NASP), or any of the single stage to orbit (SSTO) concepts being considered require advanced computational modeling to define vehicle and propulsion system performance over the nominal flight envelope and to test sensitivities to off-nominal conditions. Computational Fluid Dynamics (CFD) is unique in its ability to predict complex three-dimensional flows associated with vehicles and their propulsion systems. Judicious application of CFD in the design cycle can minimize test requirements, aid in designing better tests, and help to better interpret test data. Additionally, CFD can be used effectively in extrapolating to new operating conditions for which no test capability exists. Thus, CFD is playing an increasingly important role in the design of new space vehicles and their propulsion systems. CFD codes have to be systematically validated to increase confidence and reduce risk in their use for

design and analysis. The subject of CFD code validation is gaining recognition as a topic of importance and has been the subject of several recent publications<sup>(1-9)</sup>.

CFD at Rocketdyne is a key analysis tool, regularly used in the engineering design process. Five major CFD codes have been applied to a variety of problems on major programs such as the Space Shuttle Main Engine (SSME), the National Launch System (NLS), and the National Aero-Space Plane (NASP). CFD results are regularly used as the basis for design decisions. Thus, code validation is of considerable interest. This broad range of experience has provided insight into the practical issues surrounding CFD code validation. Some observations and key lessons learned are summarized below:

- 1) A general code validation procedure for all codes and applications can be developed.
- 2) Specific, quantitative evaluation criteria are highly application dependent and it is not possible to define a single general set of validation criteria.
- 3) Quantitative validation is only meaningful within limited classes of applications.
- 4) The level of validation appropriate depends on the intended use of the CFD predictions.
- 5) The validation process must be realistically achievable within the engineering environment. In this environment, pressure to apply a code and produce results before validation is complete may be significant. Thus, the validation process must be flexible, allow for varying levels of validation, and incremental improvement as time and funding permit.

The objective of this effort is to define a comprehensive procedure with associated criteria through which all aspects of CFD codes can be validated in a consistent manner. These aspects include basic programming, solution methodology, code numerics, and physical models, as applied through the integrated CFD code. The goals of this approach are to improve and quantify understanding of the CFD code predictive capability, to establish consistent application techniques within classes of

similar problems, and to increase confidence in the use of CFD tools for engineering problems.

This contract report includes general discussion on the topic of CFD code validation. Code classifications are defined, directly relating use of CFD codes to engineering design. Evaluation criteria are developed and, because code validation depends on comparisons of CFD predictions with experimental data, criteria for experiments are also outlined. A four phase CFD code validation procedure is recommended and described in detail. Finally, the code validation procedure is demonstrated by applying it to REACT (Rocketdyne Elliptic Analysis Code for Turbomachinery).

### **1.1 Code Validation Classifications**

A primary goal of this effort is to encourage consistent application of CFD codes in engineering design. This will result in increased confidence in the use of these tools and reduce associated risks. However, CFD methods can be effectively applied with widely differing levels of accuracy. Early in the design cycle, during the conceptual definition phase, demands placed on the code may be limited to proper prediction of qualitative trends. Late in the design cycle, during the detailed design phase, extensive demands may be made of the codes, requiring detailed and accurate flowfield prediction.

Validation may be time consuming. In the engineering environment, pressure may be strong to apply a code before it is thoroughly validated. It is appropriate that a range of code validation be allowed to accommodate engineering needs. CFD codes validated according to defined procedures may be classified based on demonstrated capabilities. Once classified, codes should be applied only within these limits.

Mehta<sup>(1)</sup> defined five classifications for validated codes. To meet engineering needs, a simplified approach is proposed defining three levels of code validation.

- 1) Conceptual Design-Validated Code. Before a code can be considered validated for use in conceptual design, the following conditions must be met:

- a. Basic code methodology must be reviewed and considered relative to the end application.
- b. A study of code operability, exercising all options relevant to the end application must be conducted.
- c. A systematic determination of numerical accuracy must be completed along with successive grid refinement studies.
- d. Physical models to be employed in the final application must be quantitatively verified through comparison with data from benchmark experiments.
- e. The entire code must be exercised to demonstrate on simple, but relevant problems the ability to produce proper qualitative results.

With completion of these activities the code may be considered to be conceptual design-validated. The range of applicability is restricted to a class of problems similar to that for which the validation was conducted. Extension to significantly different problems (e.g., involving new physics) requires further validation for parts of the code not previously verified.

2) Preliminary Design-Validated Code. For a code to be considered validated for use in preliminary design activities all of the conceptual design validation requirements outlined above must be met. Additionally, the following conditions must also be met:

- a. Computed results for problems similar to that of interest must quantitatively agree with experimental data. Global performance quantities computed from CFD results must show a level of agreement consistent with established evaluation criteria. These criteria depend on the end application and must be established by those using the computational results (i.e., analyst and designer).

- b. The accuracy and limitations of experimental data used for comparisons must be known and well understood.
- c. Effects of grid distribution on prediction of global performance quantities must be established.

With completion of these activities the code may be considered to be preliminary design-validated. The range of applicability is restricted to a class of problems similar to that for which the validation was conducted. Extension to significantly different problems requires further validation.

3) **Detail Design-Validated Code.** A code is considered to be validated for use in detailed and final design activities if, in addition to satisfying all qualifications set forth in 1 and 2 above, the following conditions are met:

- a. Comparisons of computed results with available hardware test data show that the code is able to adequately model all physical effects relevant to the problem of interest.
- b. Effects of grid density on the prediction of detailed flowfield and surface quantities must be established.

With completion of these activities the code may be considered to be detail design-validated. The range of applicability is restricted to a class of problems similar to that for which the validation was conducted and extension to significantly different problems requires further validation.

## **1.2 Code Evaluation Criteria**

Evaluation criteria are the metrics against which a code is judged. These criteria can be customized according to the above defined code validation classifications to provide the degree of confidence required for each phase in the engineering design process (conceptual, preliminary, detail design). Once a code has been classified at a given level, it can then be used confidently within that phase of the design cycle.

Ideally, end users would construct a complete set of criteria to meet their needs over all design phases. For example, key criteria would be identified and quantified for each validation phase. Table 1 represents the necessary information generically.

### 1.3 Error Assessment

Errors associated with CFD codes can arise from many sources. These include code logic, numerical methods, and physical models (e.g., turbulence, chemistry). These errors need to be systematically identified, understood and, where possible, reduced before CFD can be used confidently.

Various measures can be taken to check the code logic. Independently programmed, but logically identical modules can be substituted and cross-checked. Grid studies can be conducted to ensure that successive refinement produces a correct grid independent solution. Consistency checks can be performed for established physical properties such as symmetry (e.g., does an airfoil of symmetric section at zero angle of attack produce lift). These checks are incorporated into early phases of the proposed validation procedure.

**Table 1. Generic Representation of Criteria for Three Validation Phases**

Criteria	Validation Phase		
	Conceptual	Preliminary	Detail
A	Qualitative	10%	5%
B	Qualitative	20%	10%
C	10%	5%	2%

Errors associated with numerical methods are inherent in every computational methodology. Discretization errors are associated with having a finite number of grid points, truncation, and coordinate transformation. Errors are also associated with the solution algorithm, generally an iterative procedure, and incomplete convergence. For this type of error, comparisons with an exact analytical solution may provide more insight than comparison with experiments. Comparison with high quality experimental data is, of course, the ultimate test of a code, but

Errors associated with numerical methods are inherent in every computational methodology. Discretization errors are associated with having a finite number of grid points, truncation, and coordinate transformation. Errors are also associated with the solution algorithm, generally an iterative procedure, and incomplete convergence. For this type of error, comparisons with an exact analytical solution may provide more insight than comparison with experiments. Comparison with high quality experimental data is, of course, the ultimate test of a code, but should only be done after numerical errors have been identified, understood and, where possible, reduced.

Discretization error represents the difference between a well converged solution of the discretized equations and the exact solution. Discretization error (for complex flowfields) can be quantified by either obtaining an "exact" solution through successive grid refinement (usually an expensive and time consuming task) or by using Richardson's method that expresses the error as a Taylor series in a parameter,  $h$ , representative of the grid size. It can be shown that for first order accuracy the error,  $\epsilon_h$ , between two grids  $h$  and  $2h$  (a grid twice as coarse), can be estimated as,

$$\epsilon_h \approx \phi_h - \phi_{2h}$$

where  $\phi$  represents the converged solution for a given grid. For a second order solution the error becomes,

$$\epsilon_h \approx \frac{\phi_h - \phi_{2h}}{3}$$

Prudent use of grid sensitivity studies combined with the Richardson method can be successfully used to estimate errors due to discretization.

Most methods used in CFD utilize iterative procedures. Typically, iteration is stopped when the difference between two successive iterates, measured by some norm, is less than a preselected level. Unfortunately, the convergence error, defined as the difference between the current iterate and the exact solution of the discretized equations depends not only on the difference between successive iterates, but also on the rate of convergence. It is possible to derive an expression for the error and use

this as the basis of a convergence criterion. It can be shown<sup>3</sup> that the error  $\epsilon$  is a function of the principle eigenvalue,  $\lambda_1$ , as well as the difference between two successive iterates,  $\phi^{n+1}$  and  $\phi^n$ ; this is given as,

$$\epsilon^n \approx \frac{\phi^{n+1} - \phi^n}{\lambda_1 - 1}$$

where  $\phi$  represents the solution. Various parameters can be used as  $\phi$  to monitor convergence. These parameters may either be taken directly from the solution or calculated. The choice is application dependent.

Finally, errors associated with physical modeling (turbulence, chemistry) must be addressed. These are typically the most difficult to identify and reduce. While it is generally accepted that the Navier-Stokes equations are applicable to continuous fluid physics, the ability of CFD to predict complex flow physics may strongly depend on modeling of turbulence and chemistry effects. Therefore, the range of application for a particular CFD code is limited by the physical models employed. Careful quantification of physical model limitations must be carried out. Comparison with benchmark experiment data should be performed relatively early in the validation process.

#### **1.4 Criteria for Selection of Code Validation Experiments**

For all but the most fundamental flow cases experimental data provide the only means for evaluating whether CFD solutions are correct or not. Further, these data provide the only means for assessing an absolute level of agreement between CFD and the true flow physics. Because of this dependence on experimental data it is essential that experiments selected for CFD code validation be of the highest quality possible. Settles and Dodson<sup>(9)</sup> divided criteria for selecting validation experiments into two categories: "necessary" and "desirable". Experiments are first measured against the "necessary" set of criteria. Those experiments that do not satisfy all of these criteria should not be used for code validation. Experiments satisfying the first set of requirements should then be judged against the second set of "desirable" criteria. The best experiments will meet all of the "necessary" criteria and should satisfy many of the "desirable" criteria. Adapting and generalizing the recommendations of Settles and

Dodson, "necessary" and "desirable" criteria are listed below, roughly in order of importance.

### "Necessary" Criteria

- 1) Applicability to Problem of Interest. Candidate experiments must be relevant to the end application. For more fundamental flows, experiments should ideally represent a single flow feature typical of the final application. For more complex flows, experiments should represent two or more flow features typical of the final application.
- 2) Well-Defined Experimental Boundary Conditions. Candidate experiments must provide sufficient and accurate information at all flow boundaries to allow accurate CFD modeling. Typical data should include detailed definition of inflow and outflow conditions including velocity distributions, pressure, temperature, total conditions (as applicable), and wall temperatures.
- 3) Well-Defined Experimental Error Bounds. The experimenter must provide a substantiated analysis of the accuracy and repeatability of the data. This error analysis should be represented through error bars on the data. Without this information comparisons between CFD and test data can not be accurately interpreted.
- 4) Self-Consistency of Data. Results from a given experiment must not be contradictory. If such results are found, they must be either resolved, preferably through direct contact with the experimenter, or the results should not be used for CFD code validation.
- 5) Adequate Documentation of Data. Experimental data must be documented with sufficient detail and clarity to allow for direct numerical comparisons. Data should be available in a tabular form that can be easily compared and cross-plotted with computational results. Data available only in the form of plots must be sufficiently legible that numerical values can be ascertained well within stated error bounds.

- 6) Adequate Spatial Resolution of Data. Data must be provided in sufficient detail to adequately resolve key flow features. This is particularly important for more fundamental flows where basic physical models within the CFD code are to be evaluated. It is recognized that for more complex flows, data are typically less available.

#### "Desirable" Criteria

- 1) Data for Physical Models. Experiments conducted with the intention of providing data on basic physical phenomena (typically represented by physical models within CFD codes) should include more than simple mean-flow measurements. Appropriate data might include Reynolds stresses or spatial distribution of chemical species.
- 2) Nonintrusive Instrumentation. Nonintrusive measurements are the preferred data acquisition technique. Characteristic of this type of instrumentation, questions of relative error are largely alleviated.
- 3) Redundant Measurements. Redundant measurements provide a means for easily verifying the "necessary" self-consistency criteria. Ideally, data should be taken to provide alternate methods of measuring key flow features and to verify basic modeling assumptions (e.g., replication of data mirrored across symmetry plane substantiates use of the CFD symmetry modeling assumption)
- 4) Flow Structure and Physics. Measurements that reveal flow structure are strongly desired. Relatively new techniques such as planar laser-induced fluorescence (PLIF) provide nonintrusive measurements in two-dimensional cuts through the flowfield. This allows for direct high level comparison of CFD predictions with spatially accurate flow measures. Visualization techniques typically used to postprocess CFD results can similarly be applied to measured data improving qualitative understanding of the flow as well.

## **2.0 CFD CODE VALIDATION PROCEDURE**

The general code validation procedure developed is described in this Section. This procedure may be used with any CFD code and can be customized for any application of interest. Because quantitative evaluation criteria are application dependent they have been uncoupled from the general procedure. The proposed validation procedure can be realistically performed within typical constraints of the engineering environment. This process is flexible, allowing for varying levels of validation to be performed and incrementally upgraded as time and funding permit.

Because the procedure must ultimately be customized for a given class of applications, requirements directly related to the end application must be identified first. One must assess the level of validation required (i.e, for conceptual, preliminary, or detail design). Appropriate criteria based on engineering design methods must be established for the selected level. These criteria will typically be expressed in terms of the level of agreement required for conceptual (qualitative trends), preliminary (global performance values), or detail design (specific flow features and values) code validation.

Having established code evaluation criteria, one must select appropriate fundamental flow cases, benchmark experiments, and quality tests against which CFD predictions can be compared. Selected cases must directly represent one or more features characteristic of the end application. To ensure this, one must study that problem and consider all relevant features. The end application is then successively decomposed into a series of less complex problems for which quality data exist.

This successive decomposition occurs over four steps as an integral part of the validation procedure. The four phase validation procedure is illustrated in Fig. 1. Phases 1 through 4 represent increasing levels in flow and geometric complexity. Phase 1 includes fundamental flows only. Phase 4 includes complex flows that directly represent the end application. Availability of data generally decreases as the flow complexity increases. Often, the quality of that data decreases as well. As one progresses through each validation phase, additional information about the CFD code, as applied to the end application, is obtained. Information learned in Phase 1 is

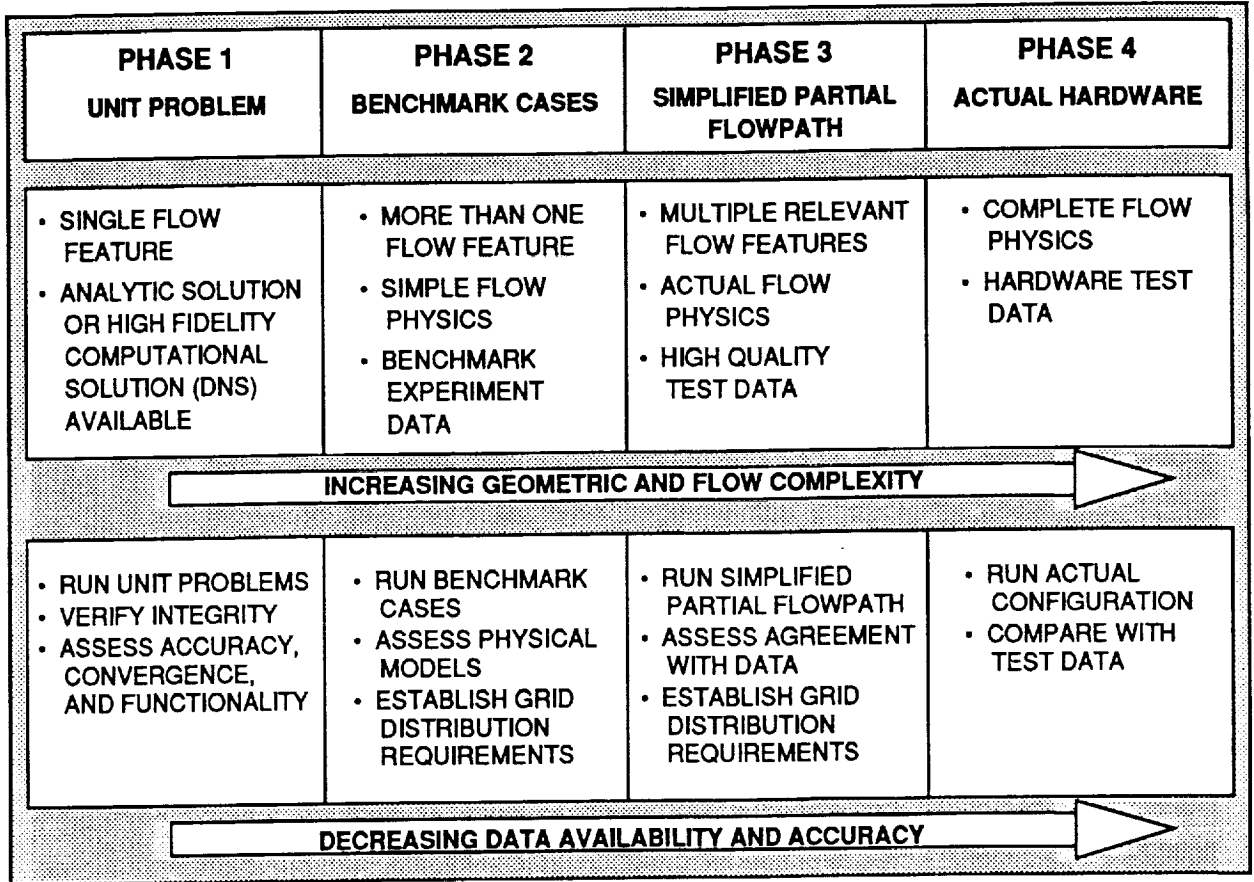


Figure 1. Four Phase Code Validation Procedure

applied in Phase 2 and so on. Ultimately, an extensive knowledge base is developed in support of the final application.

### 2.1 Phase 1 – Unit Problems

Relevant unit problems, based on successive decompositions of the end application, are identified in Phase 1. Unit problems are characterized by a single dominant flow feature and have available analytical solutions. In Phase 1, the CFD code is exercised on several unit problems, each representing one basic flow feature of the end application. This phase acts as a final code verification in which fundamental code characteristics are thoroughly understood and documented. Basic code methodology is considered in terms of its applicability to the problem of interest. All aspects of the code relevant to the end application are exercised to verify accuracy, functionality, and convergence characteristics. At least one unit problem is selected to

extensively test basic code logic through tests previously suggested (substitution of key code modules, tests for symmetry, etc.). Additionally, systematic grid sensitivity studies are conducted, both to assess relative error and to provide guidance in specifying computational grids for more complex flow cases.

## **2.2 Phase 2 – Benchmark Cases**

Relevant benchmark cases, based on successive decompositions of the end application, are identified in Phase 2. These benchmark cases are relatively simple as compared with the final application, but are characterized by more than one flow feature. Phase 2 cases should include basic physics relevant to the final application. Physical models within the CFD code are exercised to verify operability and to quantify accuracy relative to the benchmark data. Only data from the highest quality experiments should be used for comparisons with CFD solutions. Grid sensitivity studies are conducted to assess the level of refinement necessary to capture key physical effects. Error assessment techniques previously discussed are used as a guide. Lessons learned from Phase 1 should be applied to Phase 2. Overall, fewer cases will be run in Phase 2 than were run in Phase 1. A code validated through Phase 2, satisfying all established criteria may be considered validated for conceptual design studies.

## **2.3 Phase 3 – Simplified Partial Flowpath**

Test cases selected for Phase 3 are moderately complex. These cases are simplifications of the final validation case, each representing multiple geometric or flow features of the final application. Actual flow physics of the final application should be reasonably well represented by these cases. At this level of complexity, high quality data may be difficult to obtain. Data should be selected according to the criteria previously described, but these criteria may be relaxed slightly if needed. A different type of grid sensitivity study is performed during the Phase 3 validation. An assessment on the effect of variations in grid topology and grid clustering is done to provide guidance for the end application. Again, the goal is to establish grid requirements necessary to capture key physical effects. Knowledge gained in Phase 2 sensitivity studies should prove to be useful. Relatively few cases will be run

in Phase 3. A code validated through Phase 3, satisfying all established criteria may be considered validated for preliminary design studies.

#### **2.4 Phase 4 – Actual Hardware**

Cases for Phase 4 should be selected from tests conducted using actual hardware. Thus, all of the relevant geometric and physical effects should occur simultaneously. Test data may be less available and of lower quality than that of earlier phases. Selection criteria should be carefully reviewed to allow choice of the best data sets and to identify where deficiencies in the data may exist. The knowledge base developed in Phases 1 through 3 should be applied in Phase 4. The most appropriate physical models, best grid topology, and an appropriately refined grid should be used. It is likely that only one or two cases will be run in Phase 4 of the validation procedure. A code validated through Phase 4, satisfying all established criteria may be considered validated for detail design studies.

#### **2.5 Incrementally Extending Code Validation**

As a CFD code is validated to different levels for a given application or extended to new applications, a database will be developed and gradually extended. This database will include selected analytical cases, benchmark experiment data, high quality test data, hardware test data, and associated CFD solutions. Therefore, extending an existing validation effort to either the next level or for a new application is relatively easy. As depicted in Fig. 2, much of the work may already be complete and comparatively few cases may need to be run.

### **3.0 DEMONSTRATION OF THE CODE VALIDATION PROCEDURE**

#### **3.1 Code and Application Selected**

The proposed code validation procedure is fairly detailed and it is most easily illustrated by example. The following sample validation exercise was performed primarily for illustrative purposes.

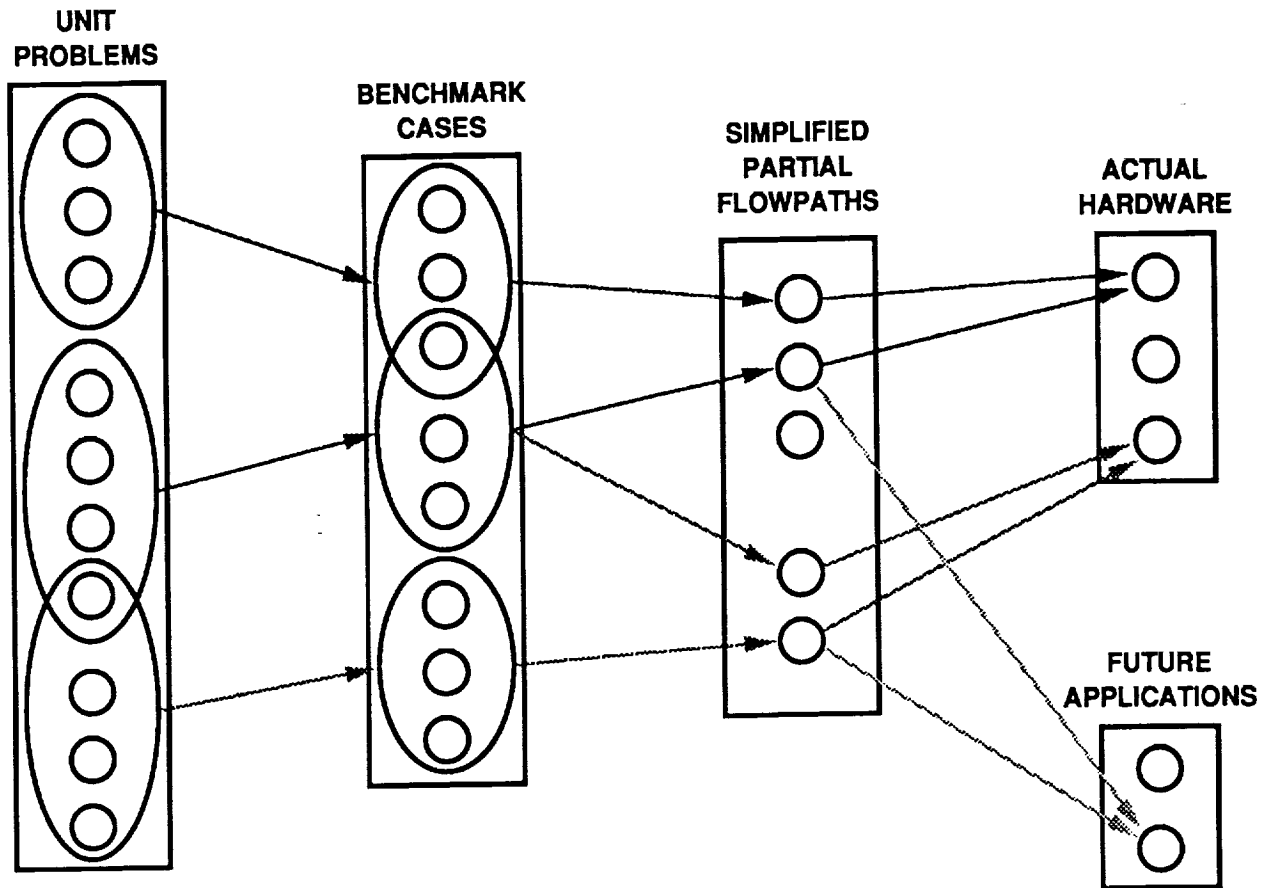


Figure 2. Building Block Approach to Develop Validation Database

### 3.1.1 Identify Code to be Validated

The evaluation procedure discussed can be used to evaluate any CFD code. REACT(10, 11, 12) (Rocketdyne Elliptic Analysis Code for Turbomachinery) was selected for this demonstration effort.

The REACT code is a general purpose 2-D/3-D full Navier-Stokes code. REACT operates in generalized coordinates and uses a second-order correct finite volume discretization scheme. Various solvers including conjugate gradient, Stone's strongly implicit procedure, and ADI techniques are available. The code offers various turbulence models such as the standard  $k-\epsilon$ , low Reynolds number  $k-\epsilon$ , and multiscale  $k-\epsilon$ . The REACT methodology is applicable for flow conditions ranging from

incompressible to low supersonic flow. The code accommodates a variety of boundary conditions including multiple inlets and outlets, planes of symmetry, spatial periodicity, and internal obstacles. Geometric complexities may be accommodated through a multiple zone approach.

REACT has been used to solve many flow problems. Solutions have been obtained for virtually every component and type of flow encountered in a turbopump including inducers, impellers, crossovers, volutes, turbine cascades, cavity flows, and bearing flows.

### **3.1.2 Select Final Application and Decompose Over Four Phases**

Rocketdyne holds a strong interest in the application of CFD to the design and analysis of turbopumps. In association with the Rocketdyne role as developer of the Space Shuttle Main Engine (SSME), a series of nonintrusive measurements were taken on a SSME high pressure fuel turbopump (HPFTP) impeller. The availability of quality data for a complex piece of flight hardware, combined with interest in turbomachinery makes this an ideal validation case. Thus, the end application was identified and the goal was set to validate REACT for impeller applications.

Figure 3 illustrates the approach of successive decomposition. Given that the Phase 4 test case is an impeller, key flow features were identified. Impellers are characterized by highly three-dimensional geometry, strong curvature, and high rotational speeds. For this impeller, there are three partial blades between the full blades (Fig. 4.).

Phase 3 cases selected represent the impeller as two types of simplified flowpaths, each less complex than the complete impeller problem, but still with multiple flow features represented in the impeller. Flow within blade passages of a shrouded impeller were conceptually simplified and represented as flow through a rotating curved duct. Flow over the partial blades was reduced to flow over a three-dimensional turbine blade cascade.

Phase 2 cases were selected by decomposing those from Phase 3. The rotating curved duct was decomposed into flow in curved non-rotating ducts and flow about a rotating disk. Flow over a 3-D turbine blade cascade was represented by turbulent

PHASE 1 UNIT PROBLEMS	PHASE 2 BENCHMARK CASES	PHASE 3 SIMPLIFIED FLOWPATHS	PHASE 4 ACTUAL HARDWARE
<ul style="list-style-type: none"> <li>• flat plate</li> <li>• straight duct</li> <li>• diffuser</li> <li>• sudden contraction (lam.)</li> <li>• backward facing step (lam.)</li> <li>• driven cavity</li> <li>• rotating concentric cylinders (Taylor-Couette flow)</li> </ul>	<ul style="list-style-type: none"> <li>• square duct with 90° bend</li> <li>• S-shaped duct</li> <li>• backward facing step (turb.)</li> <li>• orifice flow (turb.)</li> <li>• flow around confined bluff bodies</li> <li>• 2-D turbine cascade</li> <li>• rotating disk</li> </ul>	<ul style="list-style-type: none"> <li>• 3-D turbine blade cascade</li> <li>• rotating curved duct</li> </ul>	<ul style="list-style-type: none"> <li>• SSME HPFTP impeller (2 sets partial blades)</li> </ul>

Figure 3. Successive Decomposition of Impeller

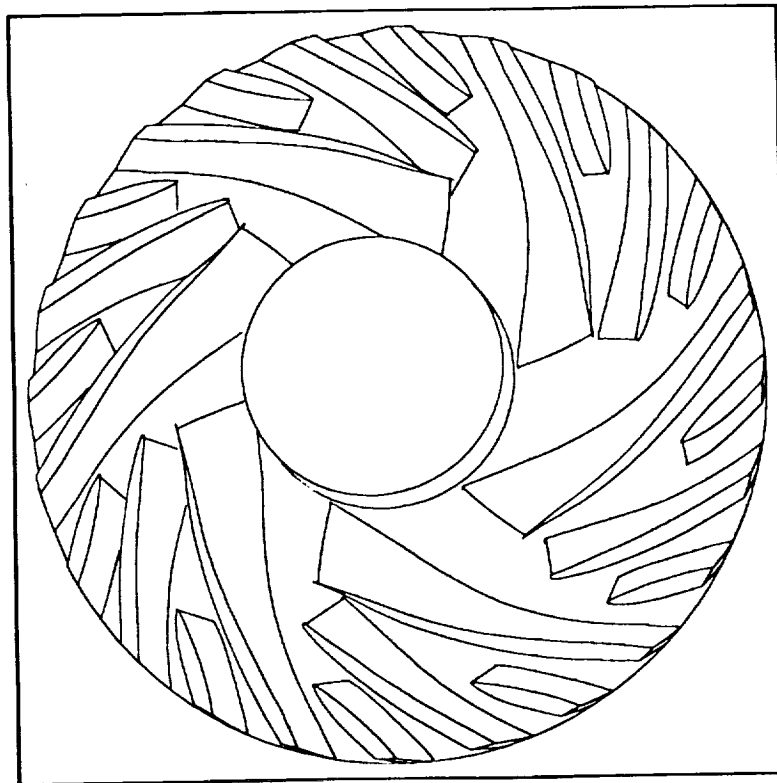


Figure 4. SSME HPFTP Impeller

flow over a variety of obstacles including backward facing steps, around confined bluff bodies, through extreme contraction and expansion of an orifice, and over 2-D turbine blades.

Finally, Phase 1 cases were selected by simplifying the Phase 2 cases one last time. The curved duct and rotating disk cases were further simplified. Straight duct flow, flow over flat plates, and fundamental cases with rotation (e.g., Taylor-Couette flow) were examined. The flows over obstacles were simplified to first look at laminar cases, removing the uncertainty of turbulence models.

Of the cases completed and represented in Fig. 3, the following were chosen to highlight various parts of the procedure:

- 1) Straight passage flow (analytic solution)
- 2) Square duct with 90° elbow (benchmark experiment data<sup>13</sup>)
- 3) SSME 3-D turbine cascade (test data<sup>14,15</sup>),
- 4) SSME HPFTP impeller (test data<sup>16</sup>).

Because Case 1 has an analytic solution, flow variables are known exactly. Test data for cases 2 through 4 include flow quantities at the boundaries. Additionally, case 2 had streamwise and radial velocity distribution measurements at several locations. Test data for case 3 also included static pressure distribution on the blade surface. An estimate of the turbine efficiency bias and precision limits was performed and was estimated to be 0.7% of the efficiency.

Test data for case 4 includes absolute and relative velocity and flow angle in several planes downstream of the impeller. The velocity measurements at the inlet plane and discharge of the impeller were completed with a L2F measurement system. This allowed for a highly accurate non-intrusive method of measuring the impeller inlet and discharge velocities. A plane approximately 1 inch upstream of the impeller was measured to provide a good inlet condition to the CFD model. Three planes downstream of the impeller were measured, these were at 5.570, 5.701, and

5.833 inches. The 5.570 inch plane was to measure the velocities just at the exit of the impeller discharge, the 5.833 inch plane was selected as this would be the standard location of the downstream component , and the 5.701 inch plane was to gain more data for validation.

Cases 3 and 4 do not strictly satisfy all requirements set for benchmark experiment standards but are representative of some of the better data available. Considering the complexity of these flows, these data sets are more than sufficient for the present purpose of demonstrating the code evaluation procedure.

### **3.1.3 Establish Code Evaluation Criteria**

The ultimate purpose of code validation is to establish a degree of confidence in the CFD code as applied in the design process. The level of predictive capability must be quantified in terms that are useful to the design engineer. For impeller design, a variety of analysis tools are employed during the course of the design cycle. Traditional (non-CFD) tools have been applied for many years over all design levels. A typical accuracy for these tools might be on the order of 10%. Consequently, test data are required for detail design and final quantification of performance.

For the conceptual design phase, CFD results must demonstrate the correct qualitative trends. Error between test data and predicted results may, for particular parameters, be large (e.g., on the order of 30%). Because the goal in this design phase is to assess the merit of one design relative to another, larger errors are generally acceptable as long as predicted trends from one design to the next are correct.

For preliminary design of an impeller, global parameters should be predicted with relatively good accuracy. Two key parameters used to quantify impeller performance are efficiency and head rise. Impeller efficiency should be predicted within 1-2% and head rise should be within about 10%. Specific flow parameters such as velocity magnitude and flow angle should be predicted within about 5% and 1°, respectively. The flow split between passages should be within 5%.

To provide detailed design data and minimize (or ultimately eliminate) the need for test data, accuracy should generally be on the order of the test data or better. Of the test

data obtained for the HPFTP impeller velocity magnitude and flow angle, error bands were quoted by the experimental group to be  $\pm 1\%$  and  $\pm 0.5^\circ$ , respectively. These values were, therefore set as criteria for CFD predictions at the detail design level. The flow split between passages should be within 2%. Agreement outside of these bands implies that, while CFD may be used for detailed design, some testing may still be required. Of the global parameters, impeller efficiency should be predicted within 1% or less and head rise should be predicted within 5% or less.

These criteria are summarized in Table 2.

**Table 2. Impeller Design Criteria for Three Validation Phases**

Criteria	Design Phase		
	Conceptual	Preliminary	Detail
Global Efficiency Head Rise	Qualitative Qualitative	1-2% 10%	<1% <5%
Specific Velocity Flow Angle Flow Split	Qualitative Qualitative Qualitative	$\pm 5\%$ $\pm 1.0\%$ $\pm 5\%$	$\pm 1\%$ $\pm 0.5\%$ $\pm 2\%$

### **3.2 Code Validation Procedures Results**

Selected results of the four code evaluation demonstration cases are presented. Phase 2, 3, and 4 calculations used the k- $\epsilon$  turbulence model. It is generally accepted that this model is sufficient to simulate turbulent flows where strong separation regions or shocks are not present.

#### **3.2.1 Phase 1 - Straight Duct**

Emphasis for Phase 1 was on verifying program logic, numerical error assessment, and the code convergence rate. It also reviews the code's capability in computing

flows using a multiple domain approach and examines a possible source of errors associated with the multizone grid approach.

Ideally, a parabolic profile should be predicted and the centerline (maximum) velocity should be twice the average. Figure 5 shows the computed streamwise velocity at the centerline of the duct outlet using both coarse and fine grids. The coarse grid solution (12 x 6 x 6) underpredicts the centerline velocity and predicts the wrong the velocity profile shape due to insufficient grid resolution. The fine grid solution (26 x 22 x 22) correctly predicted the fully developed parabolic profile with the centerline velocity at two times the average velocity. The comparison in Figure 5, clearly indicates that even for the simple straight passage flow, sufficient grid resolution is critical in correctly predicting the flow characteristics.

Two or more computational zones are often employed to model complex flowpaths. The grid must be smooth, not only within each zone, but across the zonal interfaces. The duct was regridded using two zones to study this effect. Figure 6 shows the computed centerline velocity at the duct outlet using both the single zone and two zone grids. In practice, the flow solver computes each zone separately and the information between each zone is communicated by proper interface boundary conditions. Although Figure 6 shows both approaches resulted in nearly identical velocity profiles, further examination of the flow characteristics in the full domain indicates the importance of a smooth grid distribution at the zone interface. Figure 7 shows the velocity distribution at the duct midsection using smooth and nonsmooth grid interfaces. The solution with a nonsmooth interface grid shows a local discontinuity in the velocity contours.

To further examine code logic, convergence histories were checked for single and multizone calculations. Figure 8 shows these convergence histories. The normalized residuals decrease by three orders of magnitude within twenty iterations for both calculations. Consistency between the two approaches shows the multizone approach to be logically sound.

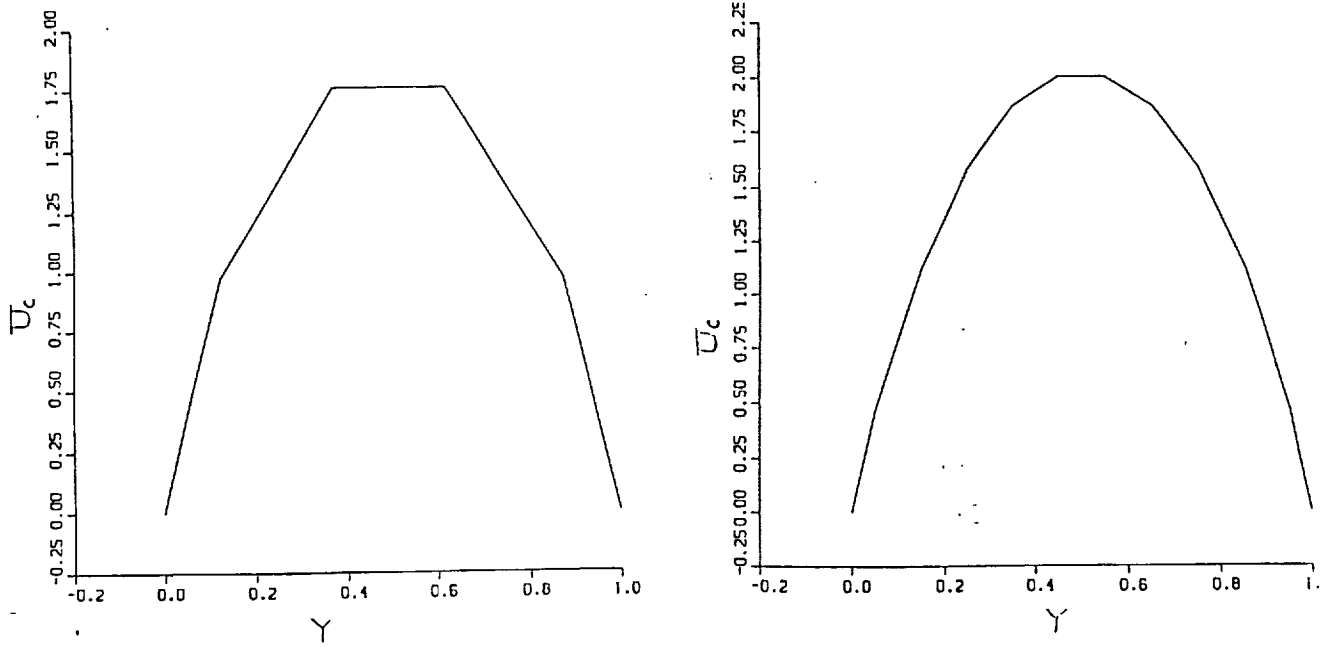


Figure 5. Streamwise Velocity Profiles for Coarse and Fine Grid Computations

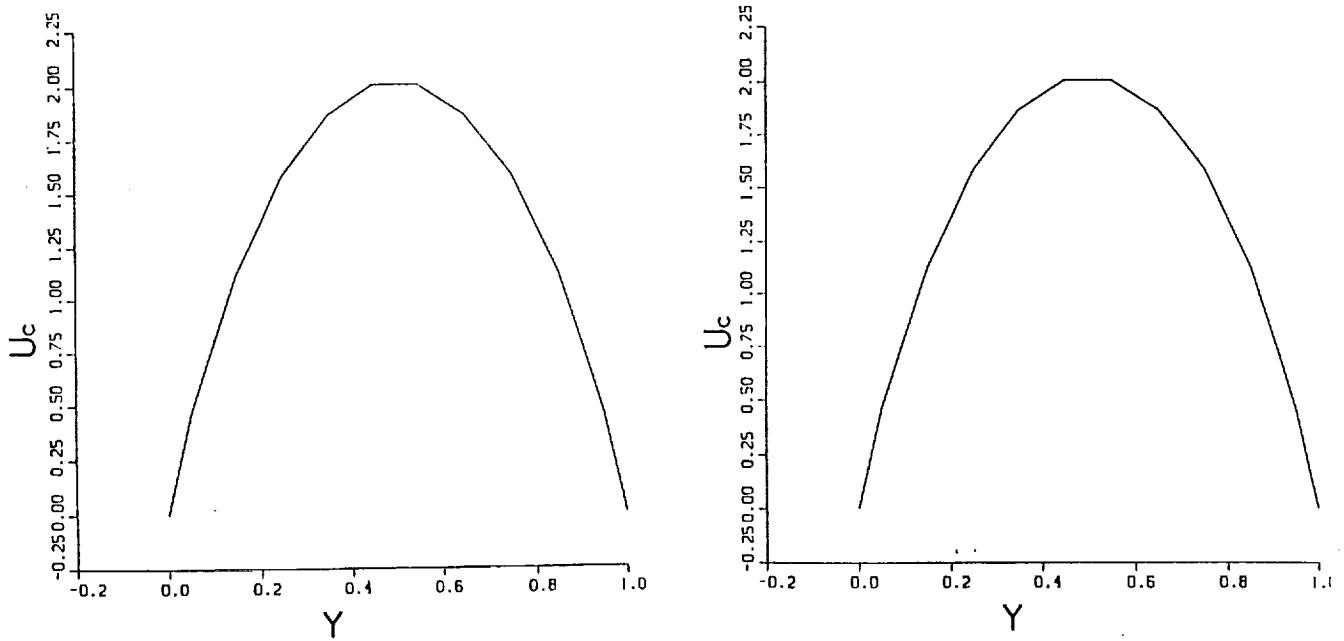


Figure 6. Streamwise Velocity Profiles for Single and Two-Zone Computations

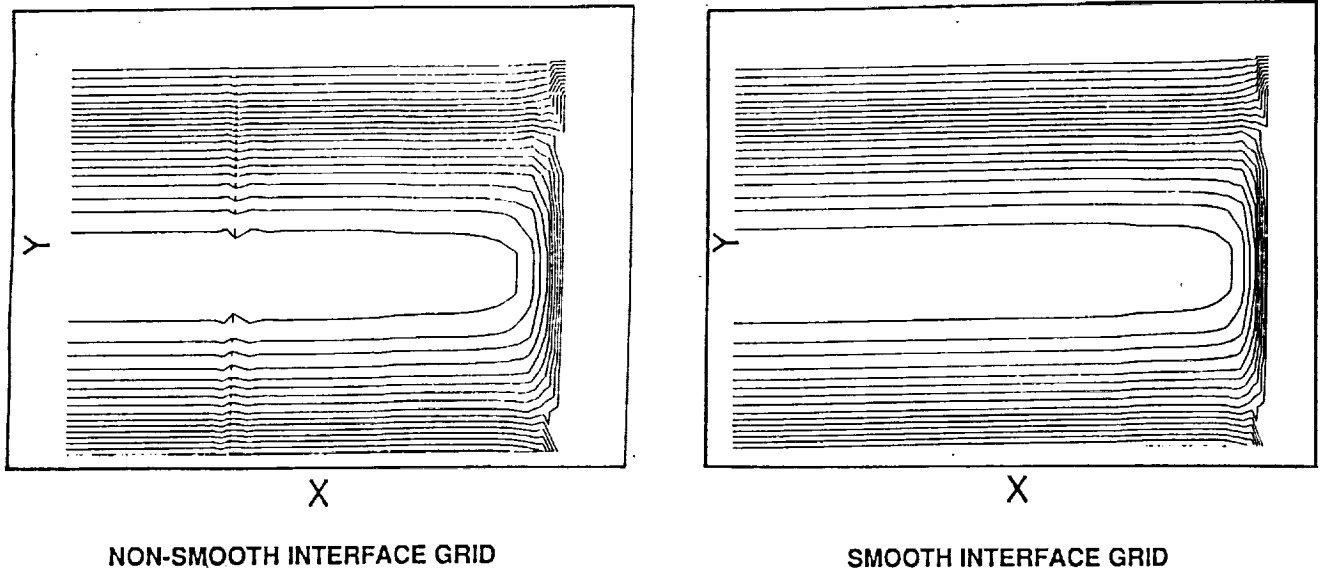


Figure 7. Velocity Contours for Nonsmooth and Smoother Zonal Interfaces

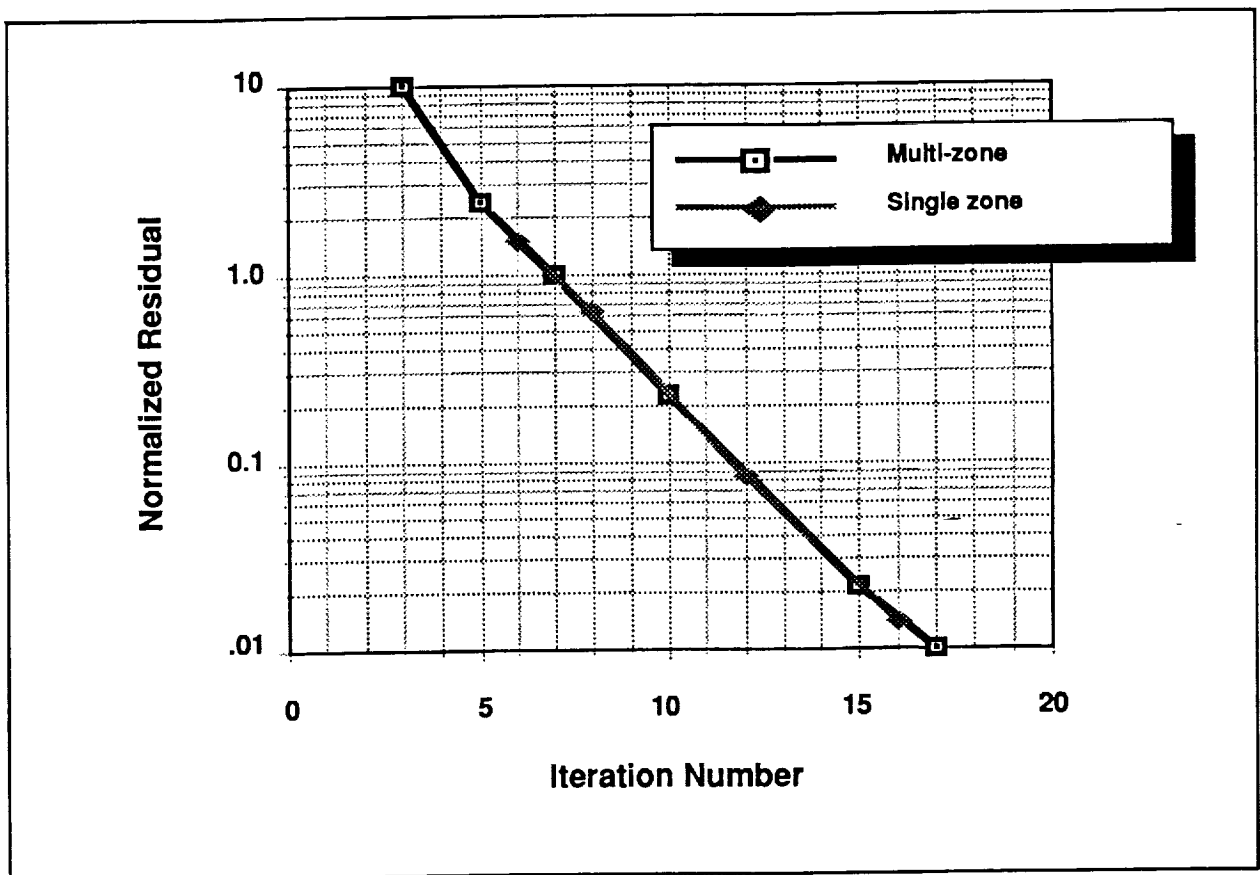


Figure 8. Convergence History for 1- and 2-Zone Duct Flow

### 3.2.2 Phase 2 – Square Duct with 90° Elbow

REACT was further validated by studying more complex flows. In this case the geometry begins to approximate that of the impeller. Complexities due to boundary layers and curvature-induced secondary flows are present. Addition of these important features increases the difficulty of accurately predicting impeller flows. Figure 9 shows the flow configuration. Figure 10 shows both the streamwise and radial velocity profiles in the spanwise direction at the 77.5° location for different radial cuts. The figure includes results of three numerical solutions with different grid distributions as compared with benchmark experimental data by Taylor, et al<sup>13</sup>. Several observations can be made:

- 1) The calculations predict the right velocity profile (qualitatively) even with the most coarse grid (88 x 22 x 12)

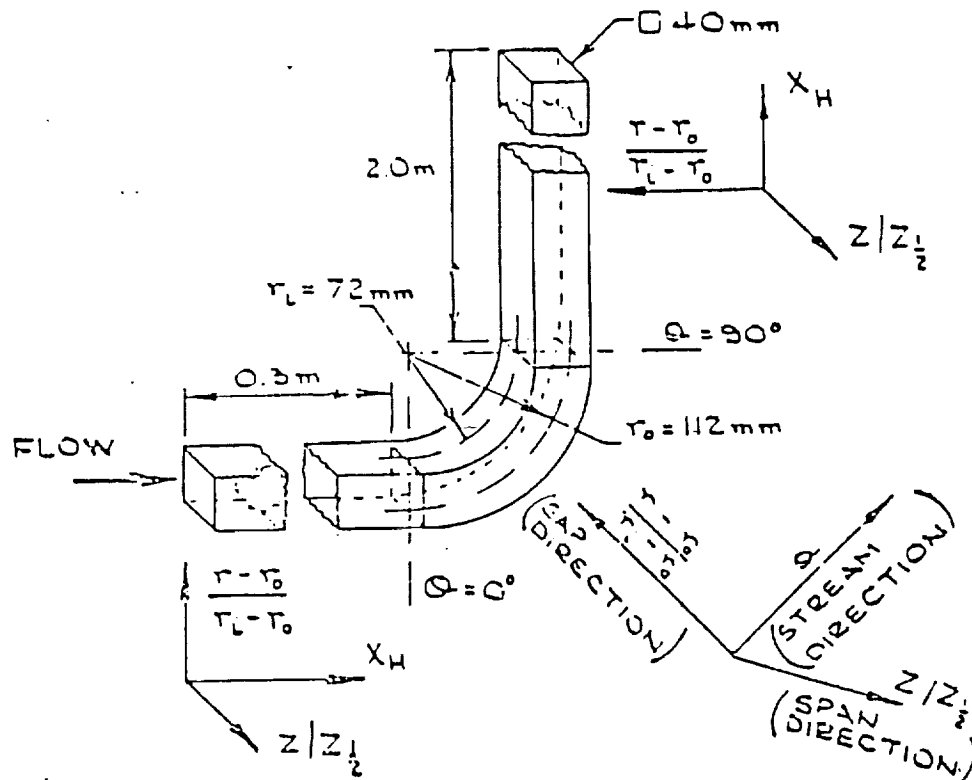


Figure 9. Flow Configuration for Square Duct with 90° Elbow



- 2) Increasing the number of grid points consistently improves agreement between the predictions and the test data
- 3) While the coarse grid solution showed large errors in some locations (on the order of 30% at radial location  $R = 0.9$ ), qualitative trends remain consistent with the data.

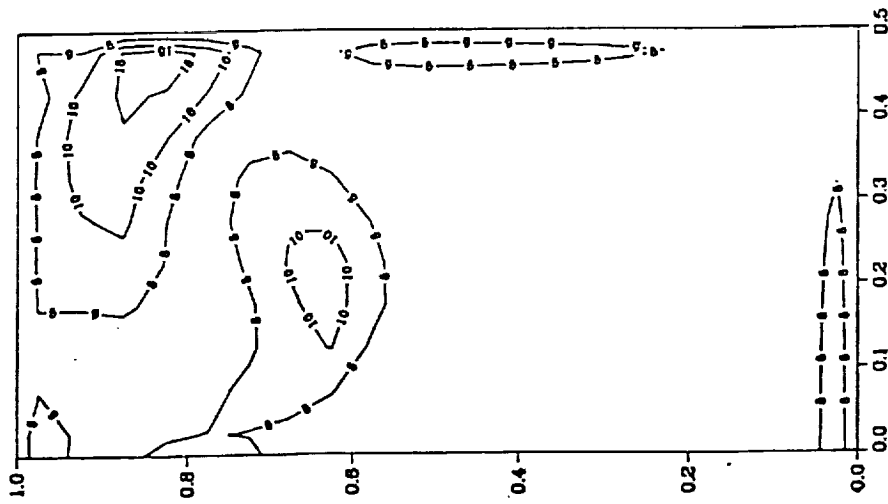
The above observations further reinforce the code's capability and consistency. It also indicates the necessity to increase the grid density to capture the secondary flow associated with curvature of the passage. Further assessment of the effect of the secondary flow can be made by studying the associated numerical error distribution. Figure 11 shows the numerical error and secondary flow distribution at the  $60^\circ$  location. The location of the strongest secondary flow is consistent with the place where the largest numerical error occurs. It indicates that the secondary flow region requires finer resolution. An additional observation can be made. Although a given grid density (for example,  $88 \times 22 \times 12$ ) may be sufficient to resolve certain flows such as a straight duct, it may not be sufficient for computing other flows accurately (such as the  $90^\circ$  elbow). Systematic evaluation of numerical results through grid sensitivity studies and numerical error assessment should be used to select the proper grid distribution to accurately compute the given flow without unnecessarily increasing computing cost.

### **3.2.3 Phase 3 – 3-D Turbine Cascade**

Solution of a turbine cascade flow introduces new geometric and flow complexities. Cascade flows are characterized by features such as high pressure gradients, end wall boundary layers, strong curvature, and secondary flow; many of the same flow features found in impellers.

Resolution of the flow near leading and trailing edges is important for accurate aerodynamic loading and heat transfer predictions. Two topologies, each with coarse and fine grids were studied as a part of the Phase 3 effort. 'H' grids are most often used for these calculations as they are the simplest to generate. 'H' grid computations can predict reasonably good overall static pressure distribution, but accuracy usually

**Estimated Error of Streamwise Velocity  
Between 88x44x22 and 88x82x42 Grids**



**Secondary Velocity Predicted  
with 88x82x42 Grid**

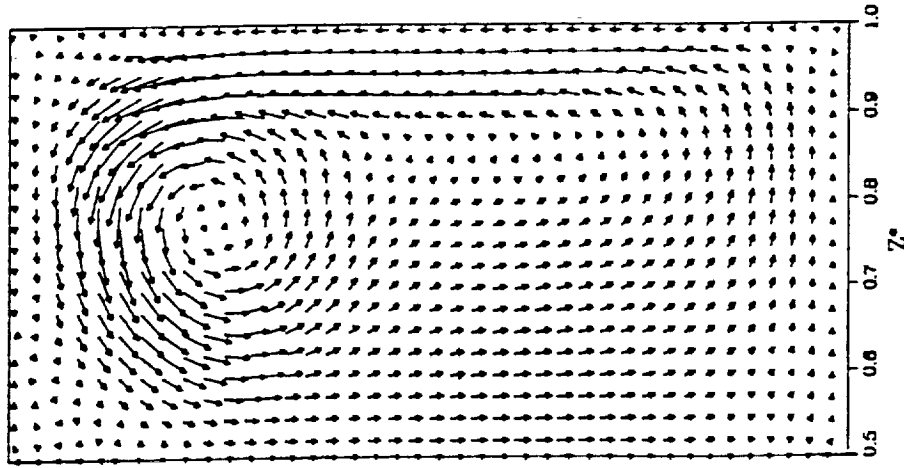


Figure 11. Numerical Error and Secondary Flow at 60° Location

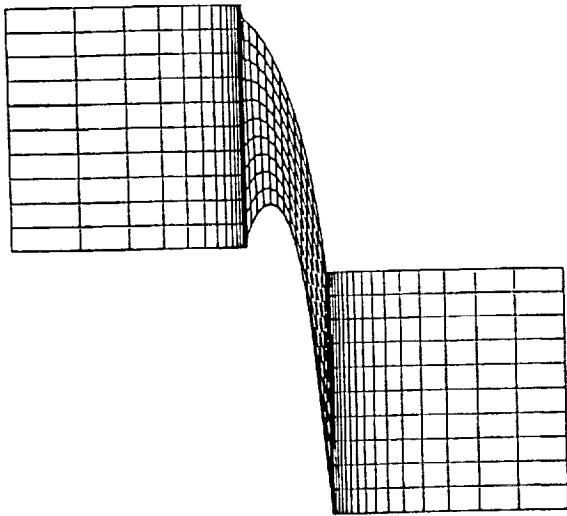
deteriorates in leading and trailing edge regions. A more elaborate 'O-H' grid topology was explored to help resolve this problem. A multiple domain grid was constructed using an 'O' grid to enclose the blade surface (helping to resolve the leading and trailing regions) and an 'H' grid outside. Construction of the multizone grid and making associated changes in the flow solver require additional effort, but do pay off in terms of increased accuracy. Figure 12 shows the single and multiple zone grids used for the SSME turbine blade.

Figure 13 shows the static pressure distributions on H and O-H grids. In both cases the grid number used was 20 x 12 x 6. The multiple zone (O-H grid) calculation shows better agreement with test data. To evaluate grid sensitivity and performance error assessment, finer grid systems were constructed by doubling the grid number used in both streamwise and circumferential directions. While both the single zone and multizone solutions show improved agreement with test data (Fig. 14), the multizone O-H grid system appears to provide consistently better predictions.

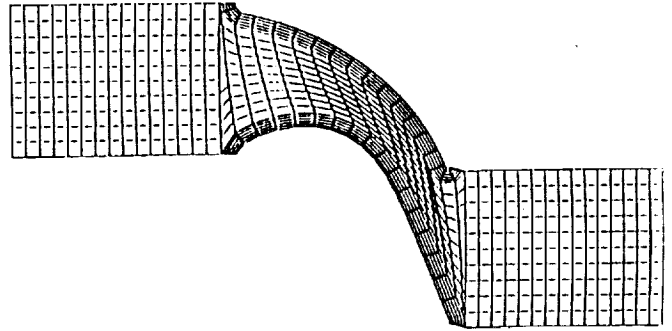
#### **3.2.4 Phase 4 – SSME HPFTP**

Impellers are highly three-dimensional. Flows are dominated by strong curvature effects, high rotational speeds, strong pressure gradients, end wall boundary layers, and secondary flows. Figure 4 shows the selected SSME high pressure fuel pump impeller from the space shuttle main engine. The geometry for this impeller is very complex. There are three partial blades between every two main (full) blades. In order to calculate the flow inside this impeller, a multiple zone approach was used. A six zone flow solver was programmed into the REACT3D code and a 3-D six zone grid was constructed. This calculation was restricted to the impeller itself. The downstream crossover passage and the diffuser were not included in the calculation and interaction effects between these components were not taken directly into account.

Figures 15a and 15b show 2-D planes of the impeller CFD model. Every attempt was made to include the significant features of the impeller and housing geometries. Figure 15a shows the expansion at the discharge of the impeller into the vaneless space. Figure 15b shows the blade-to-blade view of the impeller passage, note that the thickness at the discharge of the impeller vanes was maintained in the modeling. The grid generation was completed using an algebraic grid generation program

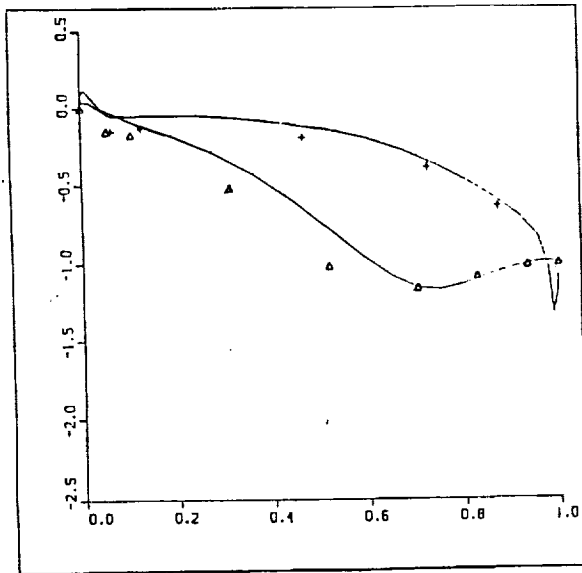


a. Typical "H" Grid

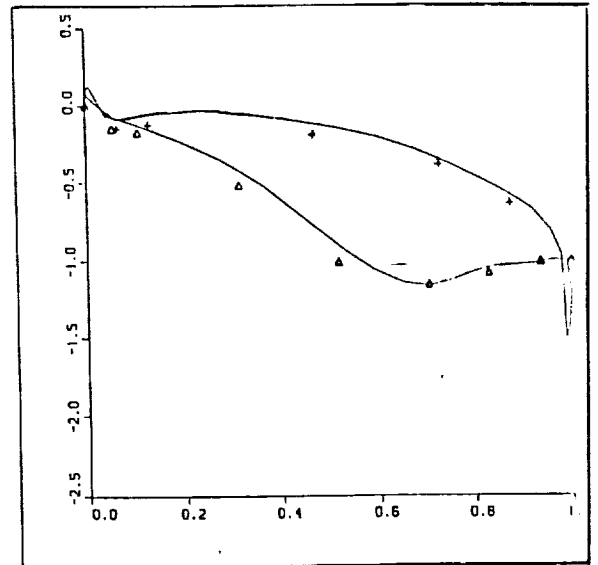


b. Modified "O-H" Grid

Figure 12. Blade Passage Grids for "H" and "O-H" Topologies

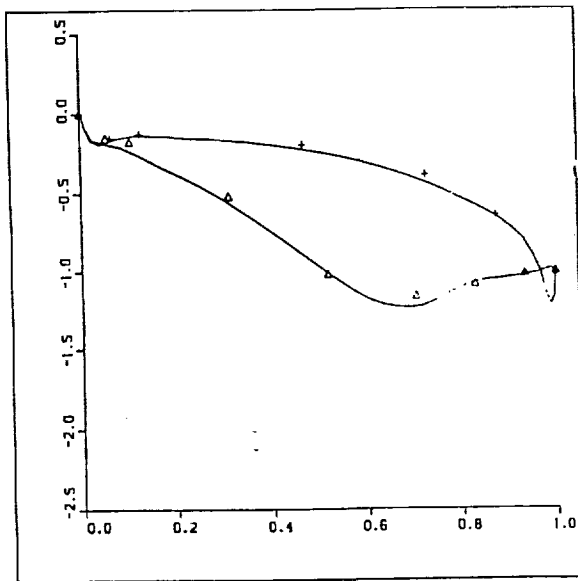


a. "H" Grid Topology

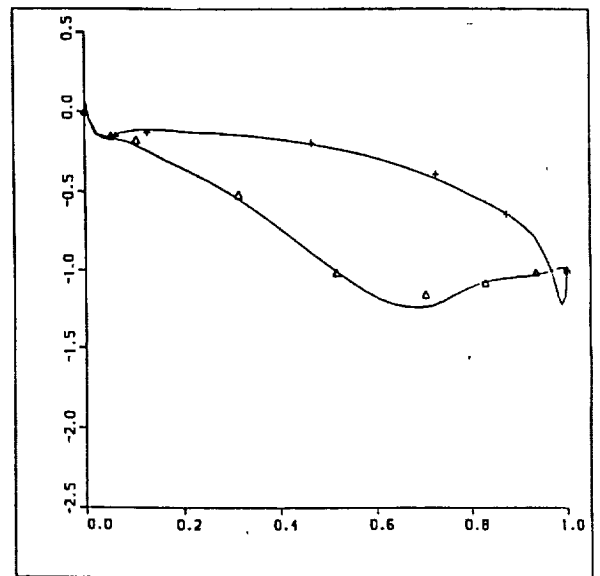


b. "O-H" Grid Topology

Figure 13. Static Pressure Distribution on Coarse Grids



a. "H" Grid Topology



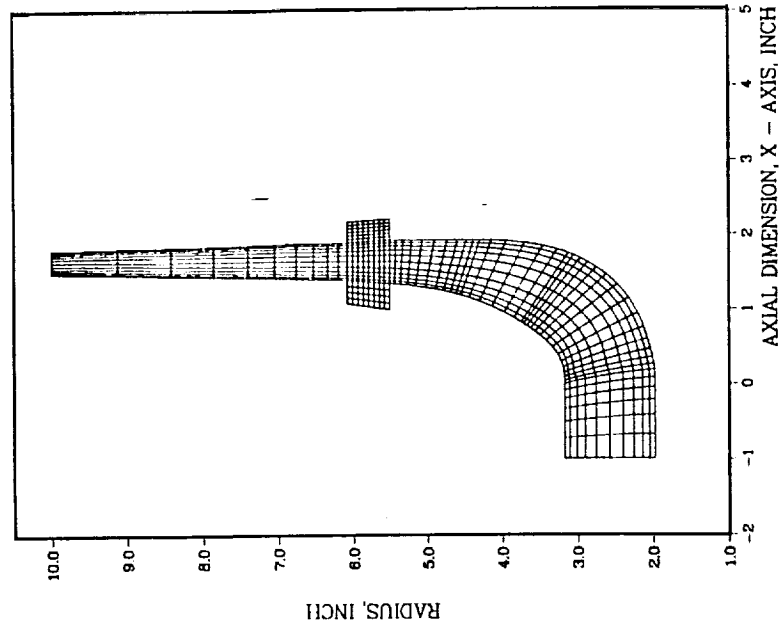
b. "O-H" Grid Topology

Figure 14. Static Pressure Distribution on Fine Grids

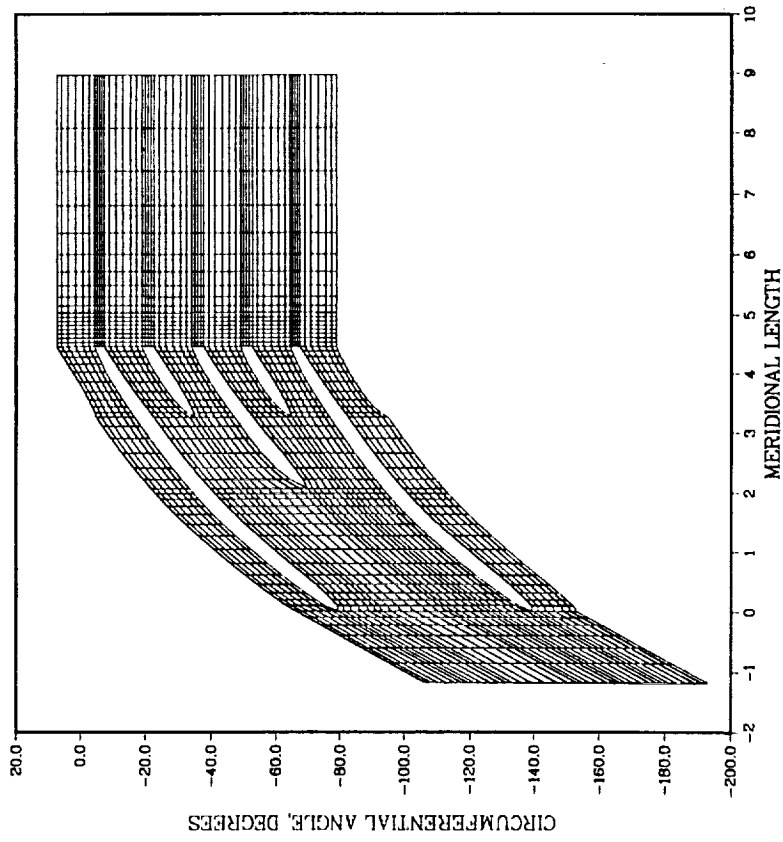
developed at Rocketdyne for the design of impellers and inducers. The generation of the 30,000 grid point and 90,000 grid point meshes took less than 3 minutes on an HP 400 workstation.

Two grid sizes were run to allow evaluation of the grid size requirement for design. The larger the grid the longer it takes to obtain a converged solution. This also allowed determination of using a small grid size for preliminary design and then a larger for more detail design applications. As a basis for time convergence time requirements, the 30,000 grid took four hours to run on a HP DN10000 workstation and the 90,000 grid took 16 hours.

The boundary conditions were set to embody the physical attributes of the impeller environment. Working from the inlet of the impeller, the boundary conditions are: stationary wall at the shroud with a small slip boundary just upstream of the impeller leading edge to mimic the gap between the stationary housing and the impeller and at



a. Radial View



b. Unwrapped Blade Passage

Figure 15. Impeller Grid Topology (30K Grid)

the hub a rotating boundary; the walls of the impeller hub and shroud as well as the blade surfaces (not shown) were considered as rotating walls; at the discharge the lower surface of the expansion contained rotating wall boundaries to model the shroud and hub thicknesses and slip boundaries to model the gaps between the impeller shroud and hub and the stationary housing; the rest of the geometry is stationary and is modeled as such.

One of the significant boundary conditions which was not modeled was the leakage flow down the hub and shroud surfaces at the discharge of the impeller. This was not done to simplify the CFD calculation. The effect of not modeling this flow is evident when the CFD results are compared with the test data.

Validation of CFD for the design of new impellers requires that the code be capable of providing a reasonable prediction of both the flow at the immediate exit of the impeller and at a plane commensurate with the location of the downstream component. The important characteristics at the immediate discharge of the impeller are the relative velocity, flow angle and flow split between the impeller blades. At the downstream component, the absolute velocity and flow angle prediction are of concern. The evaluation of the flow comparison was made for both circumferentially averaged quantities and the detail flow field. The former allows evaluation of the averaged flow characteristics and the latter evaluation determines the usefulness of the CFD solution for the prediction of dynamic loads and forcing functions on the downstream component.

Mass flow splits in each blade passage were calculated from the data and the CFD predictions. The significance of this evaluation is to provide for the design engineer an analytic capability for the placement of splitters in the flow field. Table 3 shows the results. The prediction of the flow split with both the 30,000 and 90,000 grid point models is within 1.5%. This is within the accuracy required for even detail design purposes.

Figure 16a shows the comparison of the circumferentially mass averaged relative velocity between the test data and the 30,000 and 90,000 grid point solutions at the plane immediately downstream of the impeller. The 30,000 grid point solution under

**Table 3. Impeller Flow Split Comparison**

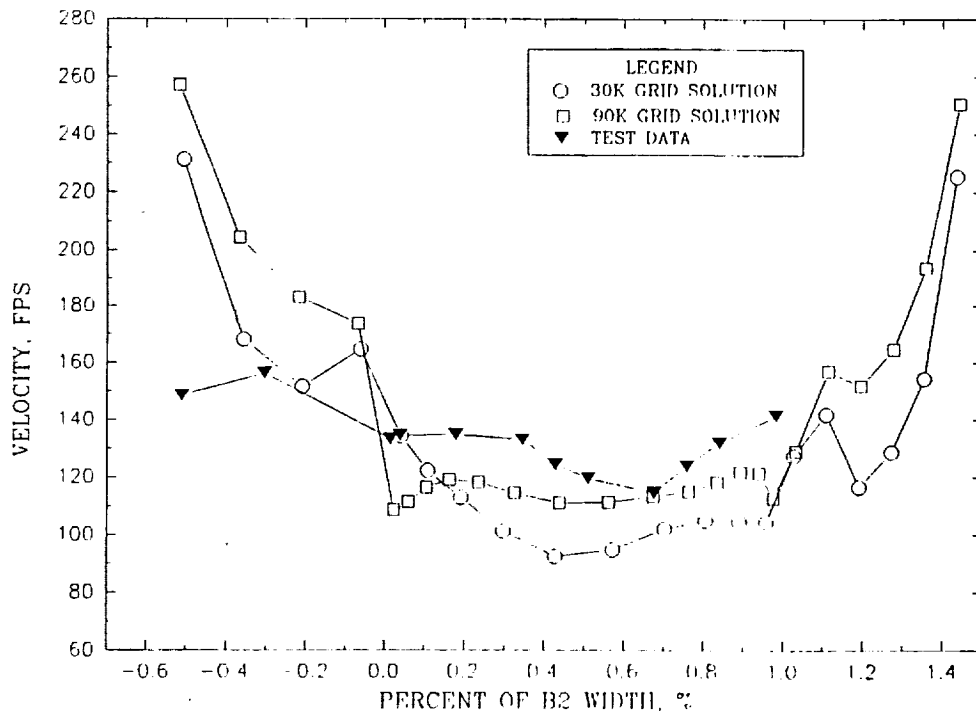
<b>Flow Branch</b>	<b>Test Data</b>	<b>30,000 Grid</b>	<b>90,000 Grid</b>
FULL Suction - Short Partial Pressure	20.84	21.31	19.68
Short Partial Suction - Long Partial Pressure	26.48	24.98	25.99
Long Partial Suction - Short Partial Pressure	24.54	25.97	25.97
Short Partial Suction - FULL Pressure	28.14	27.67	28.37

predicts the test data by approximately 30% within the  $b_2$  width region. The 90,000 grid point solution underpredicts the test data by a maximum of 15%. It can be seen that the 90,000 grid point solution is better able to predict the trend across the impeller  $b_2$  width than the 30,000 grid point solution.

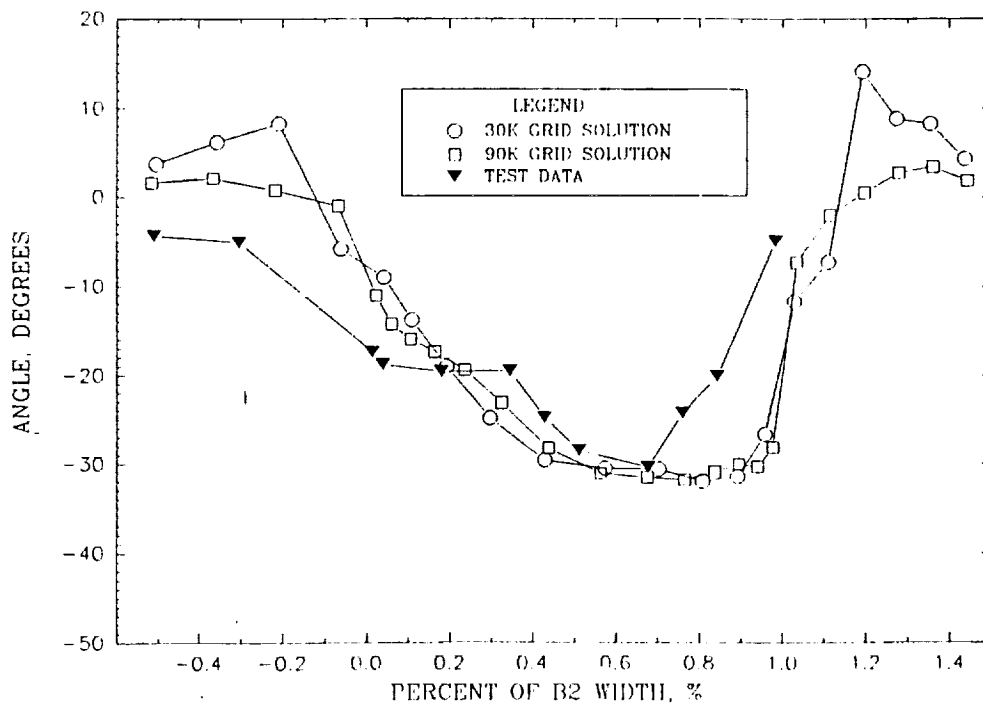
Figure 16b shows the comparison of the circumferentially mass averaged relative flow angle between the CFD solutions and the test data at the plane immediately downstream of the impeller. Although the flow angle magnitude prediction is very good within the most central region of the impeller  $b_2$  width, the magnitude correlation breaks down in the outer regions. The trend is well predicted throughout.

Figure 17a show the comparison of circumferentially mass averaged absolute velocities at the downstream plane. The prediction of both CFD solutions is within 10% for the majority of the flow domain within the impeller  $b_2$  width. The 90,000 grid solution is much better able to pick up the trends in the flow field than the 30,000 grid solution.

Figure 17b show the comparison of circumferentially mass averaged absolute flow angle at the downstream plane. The prediction is very good in both magnitude and flow angle for the entire flow region. The discrepancy in the region of the impeller shroud is attributed to secondary flows caused by the leakage down the impeller-

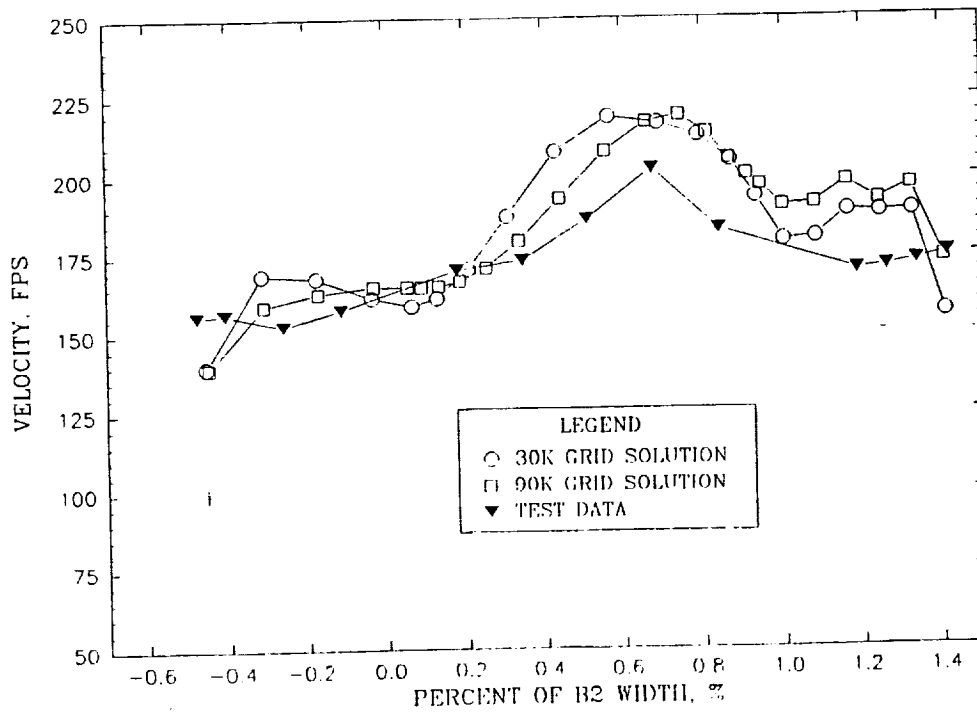


a. Relative Velocity

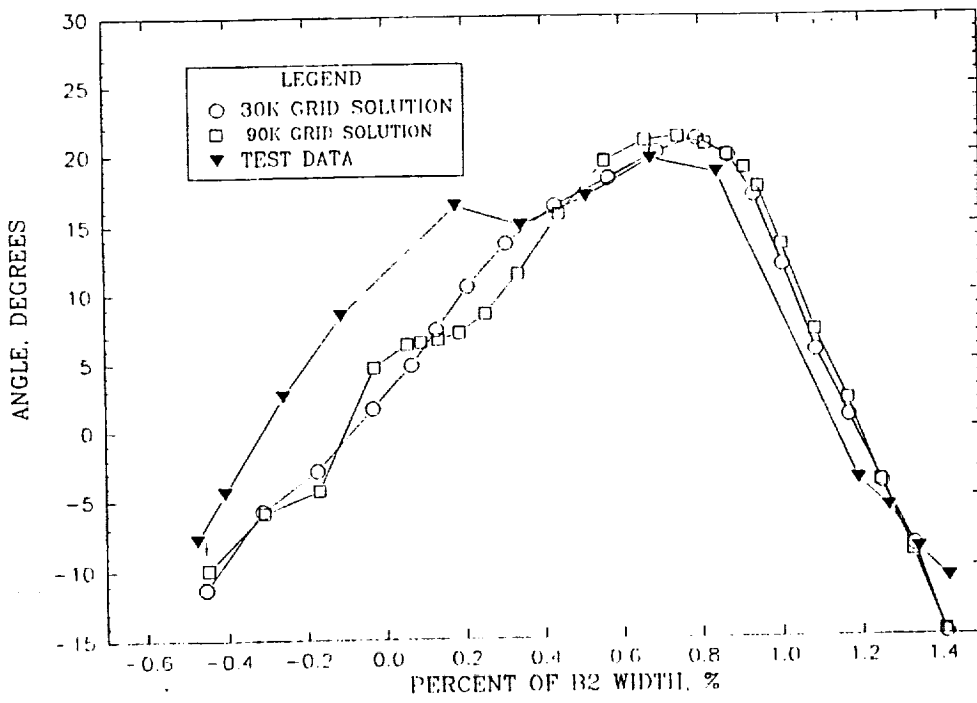


b. Relative Flow Angle

Figure 16. Comparison of CFD Solution to Test Data – Plane 1



a. Absolute Velocity



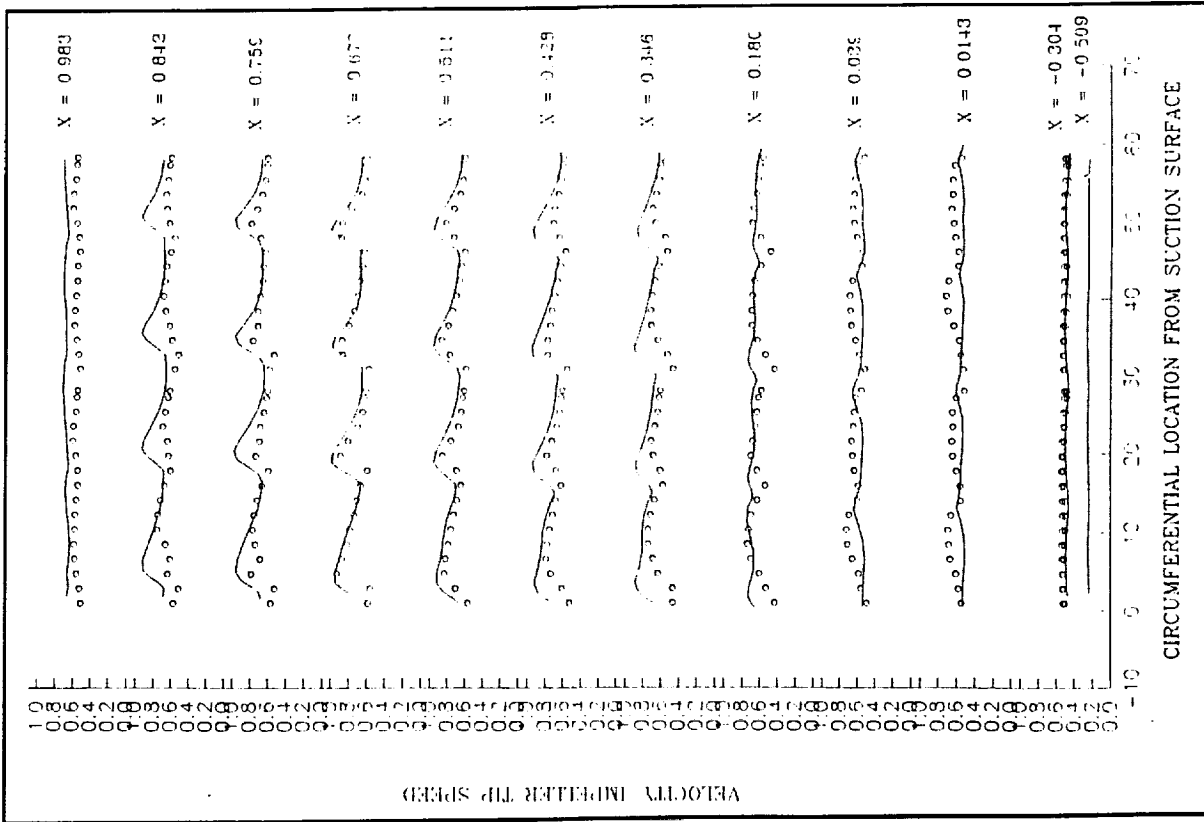
b. Absolute Flow Angle

Figure 17. Comparison of CFD Solution to Test Data – Plane 3

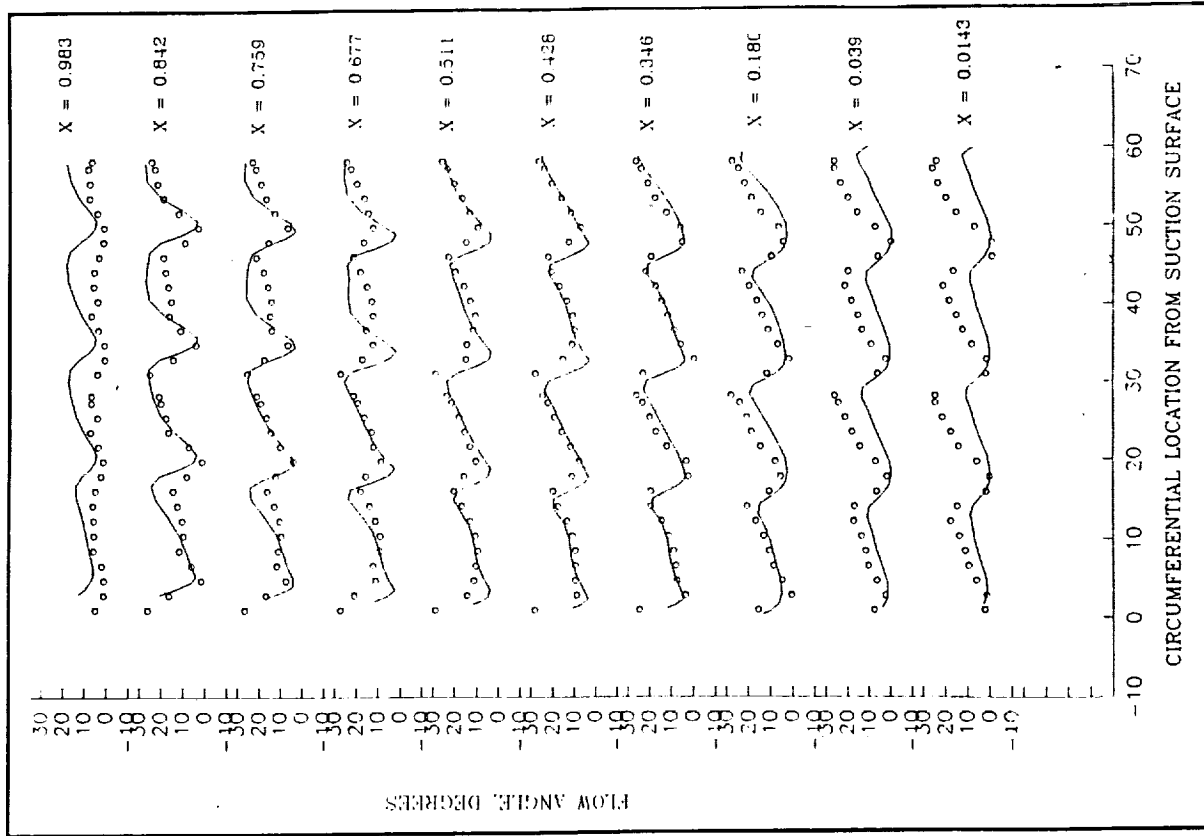
housing shroud cavity which are not modeled. Both solutions are adequate for use in design of the leading edge of a downstream component.

Figures 18 - 21 show further comparisons of test data with CFD predictions. Test data are shown for two radial locations downstream of the impeller discharge. Plane 1 is immediately downstream at a radius of 5.570 inches and Plane 3 is further away at a radius of 5.833 inches. Velocity and flow angle data are shown for various locations across these planes. The X values shown are normalized by the shroud to hub distance. The shroud is located at  $X=0.0$  and the hub is at  $X=1.0$ . CFD predictions from the 30,000 and 90,000 grid point cases are compared in each case. General observations drawn from these comparisons include:

1. Generally good agreement is achieved overall.
2. Agreement within the passage region is consistently better than that outside where wall effects are significant.
3. CFD predictions of velocity are reasonably good, particularly away from the walls. Increasing grid density improves the level of agreement. Clearly, the wake regions are missed to a large degree near the wall using the 30,000 point grid. Employing the 90,000 point grid improves agreement in the magnitude, but still misses the wake location.
4. CFD predictions of flow angle are quite good. Increasing grid density improves the level of agreement, particularly near the walls.

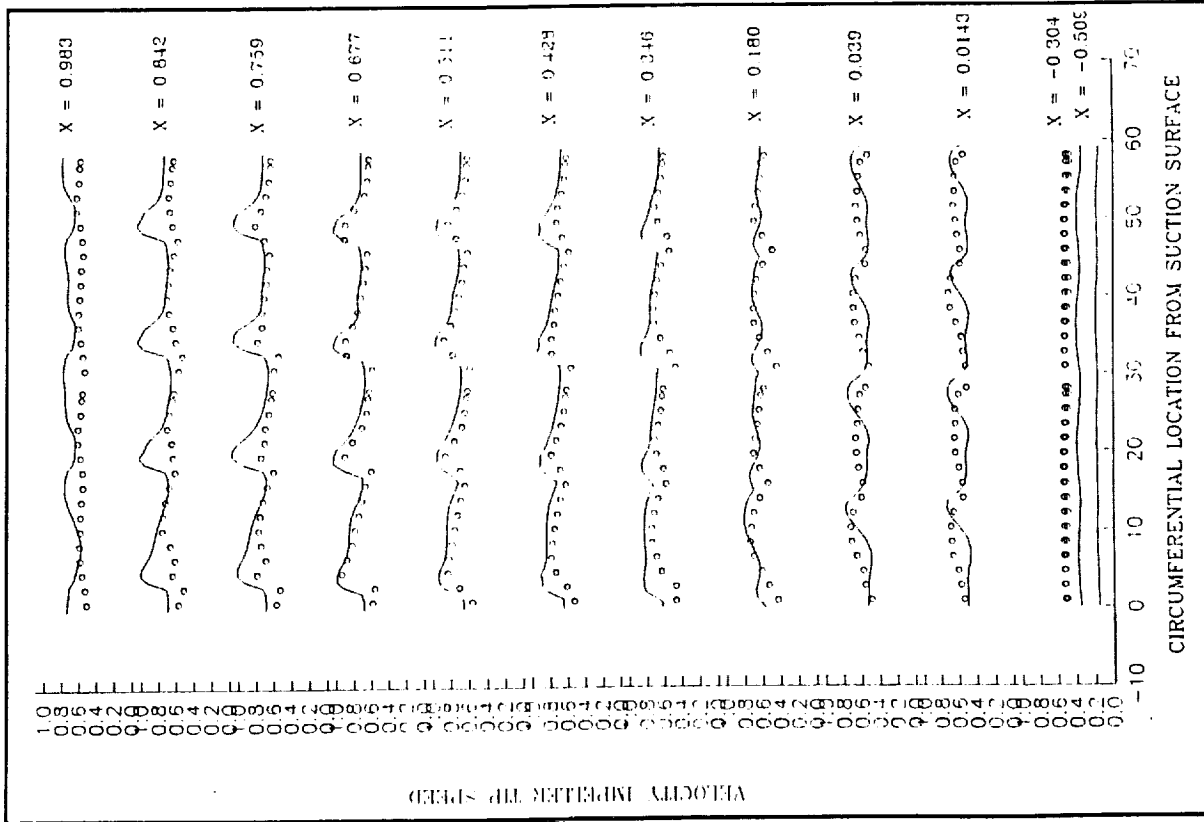


a. Velocity

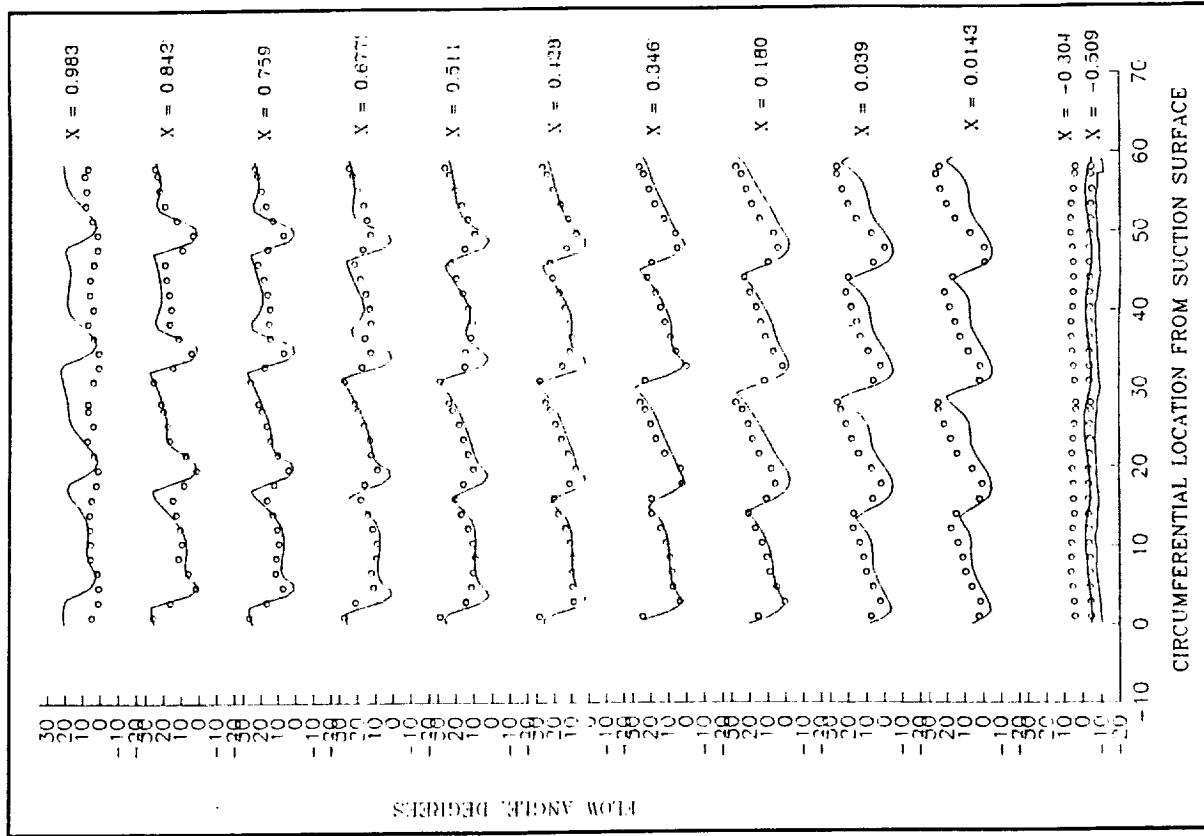


b. Flow Angle

Figure 18. Test Data versus 30K Grid Solution - Plane 1

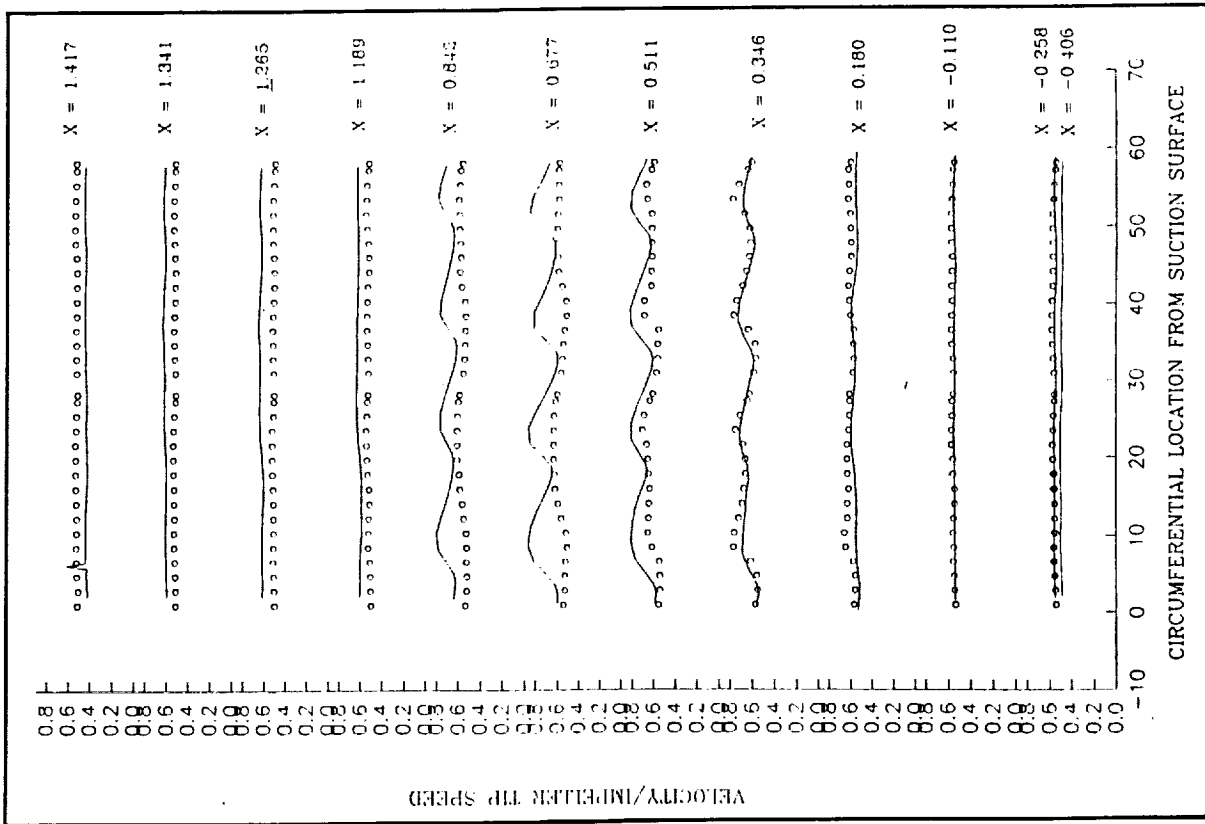


a. Velocity

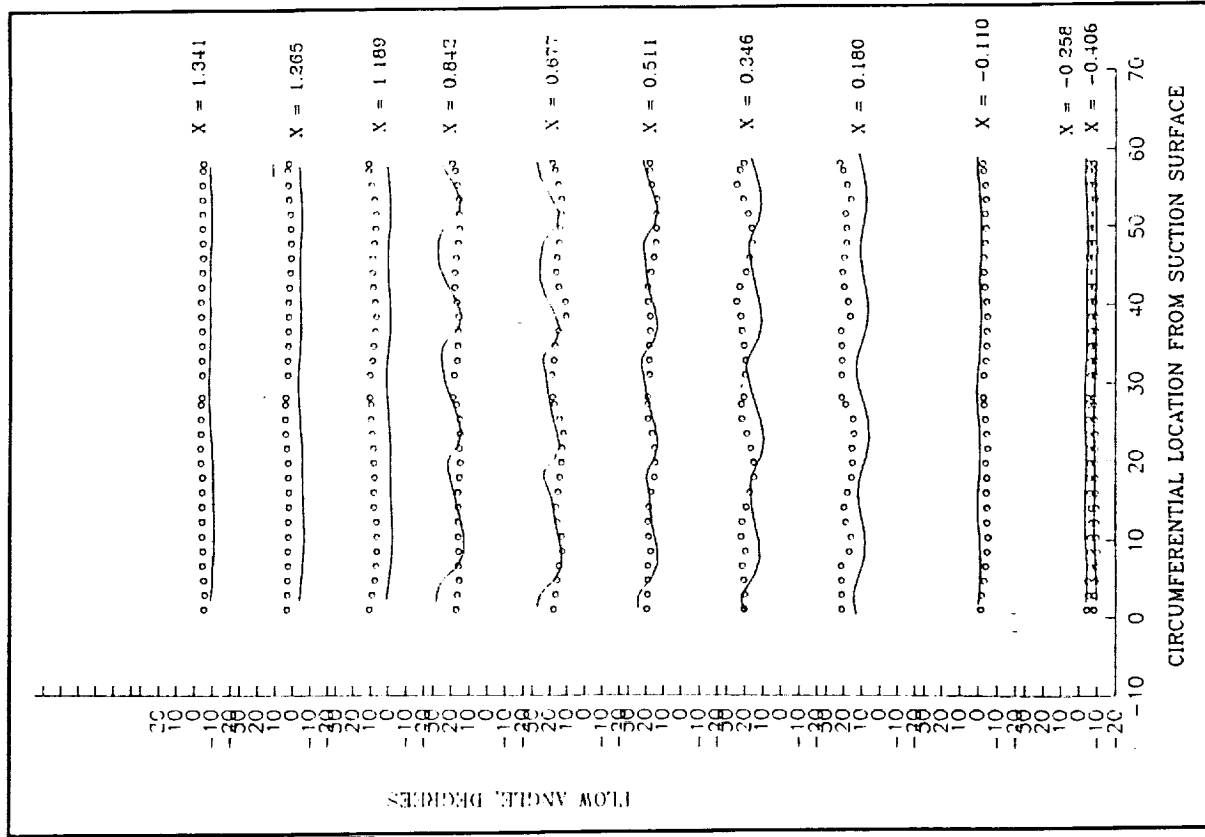


b. Flow Angle

Figure 19. Test Data versus 90K Grid Solution - Plane 1

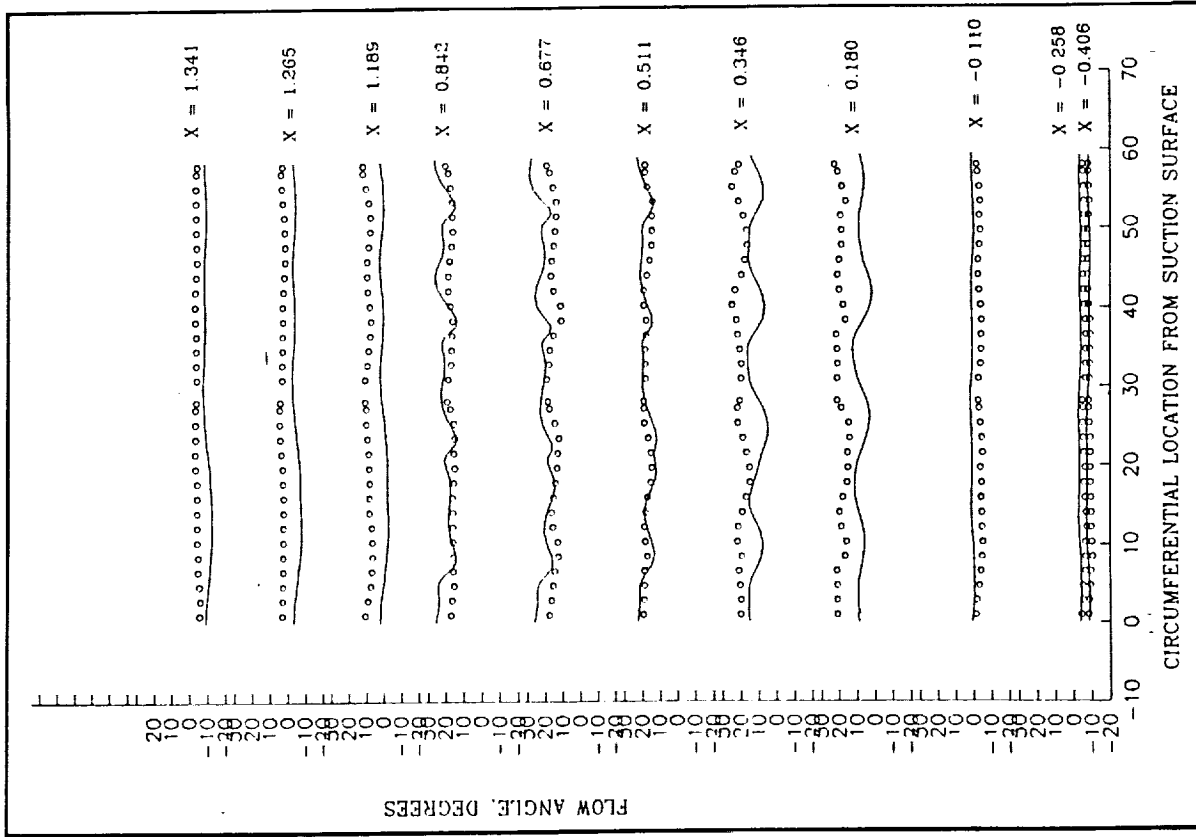
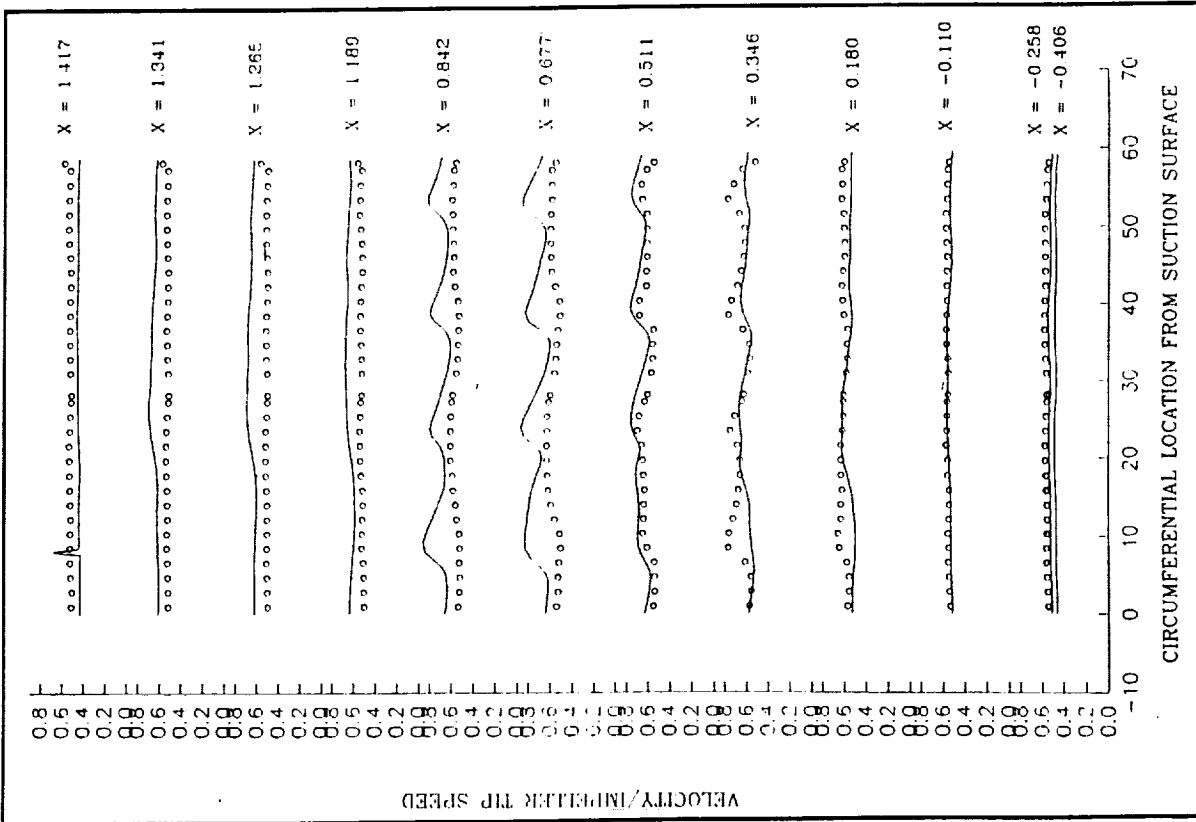


a. Velocity



b. Flow Angle

Figure 20. Test Data versus 30K Grid Solution - Plane 3



a. Velocity

b. Flow Angle

Figure 21. Test Data versus 90K Grid Solution - Plane 3

## 4.0 SUMMARY

A four phase procedure has been developed to standardize an approach for CFD code validation. The procedure is oriented toward the engineering design cycle. Three validation levels are defined to meet the needs of conceptual, preliminary, and detail design phases in the engineering environment. Detailed criteria established by the end user of the code results are used to judge the adequacy of code predictions for each validation level.

The four phase procedure outlined utilizes a series of test cases, increasing in complexity, and always with a focus on the final application of interest. Phase 1 test cases are used to assess code numerics, verify its logic, and study fundamental operability. Phase 2 tests compare code results with benchmark quality experimental data to further test the physical models and understand necessary grid requirements. Phase 3 tests code operation on flowpaths similar to the final application of interest. These flowpaths are simplified to a degree that high quality test data may be available, but contain most of the geometric and flow features anticipated in the final application. Finally, Phase 4 tests the code operability on actual hardware of interest.

The procedure has been demonstrated using the REACT code. The final application area selected was design of an impeller. Phase 1, 2, and 3 test cases were identified based on successive decomposition of the impeller flow characteristics and available test data. Ultimately, REACT was used to model the SSME HPFTP impeller. Two 3-D computations were performed using 30,000 and 90,000 grid points to represent the complete flow passage from one full blade to the next. Results were compared with extensive test data taken for the same impeller. Agreement is generally good to excellent and the REACT code has now been validated for conceptual, preliminary, and detail design of impellers.

## 5.0 REFERENCES

1. Mehta, U.B., "Computational Requirements for Hypersonic Flight Performance Estimates," AIAA, paper 89-1670, June 1989.
2. Agee, L. and Hughes, D., "Software Verification, Validation, and Quality Assurance Experiences in the Nuclear Industry," Forum on Methods for Estimating Uncertainty Limits in Fluid Flow Computations, 1989 ASME Winter Annual Meeting, December 1989.
3. Ferziger, T.H., "Estimation and Reduction of Numerical Error," Forum on Methods for Estimating Uncertainty Limits in Fluid Flow Computations," 1989 ASME Winter Annual Meeting, December 1989.
4. "Current Capabilities and Future Directions in Computational Fluid Dynamics," National Research Council, National Academy Press, Washington, D.C., 1986.
5. McCroskey, W.J., "Technical evaluation Report on the Fluid Dynamics Panel Symposium on Applications of Computational Fluid Dynamics in Aeronautics," AGARD AR-240, 1987.
6. "Symposium on Validation of Computational Fluid Dynamics," AGARD CP-437, 1988.
7. Bradley, R.G., "CFD Validation Philosophy," Symposium on Validation of Computational Fluid Dynamics, AGARD CP-437, 1988.
8. Marvin, J.G., "Accuracy Requirements and Benchmark Experiments for CFD Validation," Symposium on Validation of Computational Fluid Dynamics, AGARD CP-437, 1988.
9. Settles, G.S. and Dodson, L.J., "Hypersonic Shock/Boundary-Layer Interaction Database," AIAA-91-1763.
10. Peric, M., "A Finite Volume Method for the Prediction of Three-Dimensional Fluid Flow in Complex Ducts," Ph.D. Dissertation, Imperial College, 1985.
11. Hadid, A.H., Chan, D.C., Issa, R.I. and Sindir, M.M., "Convergence and Accuracy of Pressure-Based Finite Difference Schemes for Incompressible Viscous Flow Calculations in a Nonorthogonal Coordinate System."
12. Chan, D.C., "A Multi-Domain Computational Method for Subsonic Viscous Flows," AIAA Paper 92-3436.
13. Taylor, A.M.K, Whitelaw, J.H. and Yianneskis, M., "Measurements of Laminar and Turbulent Flow in a Curved Ducting with Inlet Boundary Layers," NASA Contract Report 3367.

14. Hudson, S.T., Gaddis, S.W. Johnson, P.D., and Boynton, J.L., "Cold Flow Testing of the Space Shuttle Main Engine High Pressure Fuel Turbine Model." AIAA-91-2503.
15. Boynton, J.L., Tabibzadeh, R., and Hudson, S.T., "Investigation of Rotor Blade Roughness Effects on Turbine Performance," The 37th ASME International Gas Turbine and Aeroengine Congress and Exposition, Cologne, Germany, Jun 1-4, 1992.
16. Prueger, G.H., Lin, S.J., Chan, D.C., and Eastland, A.H., "Validation of Computational Fluid Dynamic Analysis of a Rocket Engine Turbopump Impeller," AIAA 93-2575, Monterey, CA, June 1993.



# Report Documentation Page

1. Report No. -		2. Government Accession No.		3. Recipient's Catalog No.	
4. Title and Subtitle DEVELOPMENT OF CODE EVALUATION CRITERIA FOR ASSESSING PREDICTIVE CAPABILITY AND PERFORMANCE				5. Report Date MARCH 15, 1993	
				6. Performing Organization Code	
7. Author(s) S.J. LIN, S.L. BARSON, M.M. SINDIR AND G.H. PRUEGER				8. Performing Organization Report No. RI/RD 93-124	
				10. Work Unit No.	
9. Performing Organization Name and Address ROCKETDYNE DIVISION/ROCKWELL INTERNATIONAL 6633 CANOGA AVE., P.O. BOX 7922 CANOGA PARK, CA 91303-7922				11. Contract or Grant No. NAS8-38858	
				13. Type of Report and Period Covered - FINAL REPORT 3/91 - 3/93	
12. Sponsoring Agency Name and Address GEORGE C. MARSHALL SPACE FLIGHT CENTER NATIONAL AERONAUTICS AND SPACE ADMINISTRATION MARSHALL SPACE FLIGHT CENTER, AL 35812				14. Sponsoring Agency Code	
				15. Supplementary Notes PROJECT MONITORS, DR. PAUL McCONNAUGHEY AND MR. JOE RUF - NASA/MSFC PROGRAM MANAGER, DR. GLENN HAVSKJOLD, ROCKETDYNE DIV./ROCKWELL INTERNATIONAL	
16. Abstract <p>Computational Fluid Dynamics (CFD), because of its unique ability to predict complex three-dimensional flows is being applied with increasing frequency in the aerospace industry. Currently, no consistent code validation procedure is applied within the industry. Such a procedure is needed to increase confidence in CFD and reduce risk in the use of these codes as a design and analysis tool. This final contract report defines classifications for three levels of code validation, directly relating the use of CFD codes to the engineering design cycle. Evaluation criteria by which codes are measured and classified are recommended and discussed. Criteria for selecting experimental data against which CFD results can be compared are outlined. A four phase CFD code validation procedure is described in detail. Finally, the code validation procedure is demonstrated through application of the REACT CFD code to a series of cases culminating in a code to data comparison on the Space Shuttle Main Engine High Pressure Fuel Turbopump Impeller.</p>					
17. Key Words (Suggested by Author(s)) CFD, CODE VALIDATION			18. Distribution Statement UNCLASSIFIED - UNLIMITED		
19. Security Classif. (of this report) UNCLASSIFIED		20. Security Classif. (of this page) UNCLASSIFIED		21. No of pages 48	22. Price*